INFORMATION TO USERS

This was produced from a copy of a document sent to us for microfilming. While the most advanced technological means to photograph and reproduce this document have been used, the quality is heavily dependent upon the quality of the material submitted.

The following explanation of techniques is provided to help you understand markings or notations which may appear on this reproduction.

1. The sign or "target" for pages apparently lacking from the document photographed is "Missing Page(s)". If it was possible to obtain the missing page(s) or section, they are spliced into the film along with adjacent pages. This may have necessitated cutting through an image and duplicating adjacent pages to assure you of complete continuity.

2. When an image on the film is obliterated with a round black mark it is an indication that the film inspector noticed either blurred copy because of movement during exposure, or duplicate copy. Unless we meant to delete copyrighted materials that should not have been filmed, you will find a good image of the page in the adjacent frame.

3. When a map, drawing or chart, etc., is part of the material being photographed the photographer has followed a definite method in "sectioning" the material. It is customary to begin filming at the upper left hand corner of a large sheet and to continue from left to right in equal sections with small overlaps. If necessary, sectioning is continued again–beginning below the first row and continuing on until complete.

4. For any illustrations that cannot be reproduced satisfactorily by xerography, photographic prints can be purchased at additional cost and tipped into your xerographic copy. Requests can be made to our Dissertations Customer Services Department.

5. Some pages in any document may have indistinct print. In all cases we have filmed the best available copy.

University
Microfilms
International

300 N. ZEEB ROAD, ANN ARBOR, MI 48106
18 BEDFORD ROW, LONDON WC1R 4EJ, ENGLAND

BUNDING, KATHRYN ADELE

SURFACE ENHANCED RAMAN SPECTRA OF MOLECULES ADSORBED ON SILVER ELECTRODES

City University of New York PH.D. 1980

Surface Enhanced Raman Spectra of Molecules Adsorbed on Silver Electrodes

by

Kathryn Adele Bunding

A dissertation submitted to the Graduate Faculty in Chemistry in partial fulfillment of the requirements for the degree of Doctor of Philosophy, The City University of New York

1980

This manuscript has been read and accepted for the Graduate Faculty in Chemistry in satisfaction of the dissertation requirement for the degree of Doctor of Philosophy.

7/23/80
date

John R. Lombardi
Chairman of Examining Committee

7/23/80
date

David C. Lorke
Executive Officer

Herbert Kenschuh
William E. L. Grossman
Ronald Breslow
Supervisory Committee

The City University of New York

DEDICATION

to

ALLEN W. GIN

Table of Contents

List of Tables

List of Figures

I. BACKGROUND

Surface enhanced Raman spectroscopy (SERS) is a new phenomenon that allows detailed chemical analysis of monolayers of species adsorbed on metal surfaces. Although the phenomenon of the enhancement of Raman spectra of molecules adsorbed on electrodes was determined as recently as 1976 [1,2], the potential uses of SERS have caused this field to expand rapidly both in determining applicability and theoretical explanations.

The first report of the Raman spectroscopy of molecules adsorbed on a metal electrode surface was the note of Fleischmann, Hendra and McQuillan in 1973 [3]. This study showed that layers of Hg_2Cl_2, Hg_2Br_2, and HgO prepared by electrolytic deposition on a mercury coated platinum surface gave a Raman spectrum of the adsorbed layers. Earlier studies of an adsorbed layer at the solid/gas interface using infrared absorption [4] and Raman spectroscopy [5] had yielded information about the adsorbed species suggesting a further extension of Raman spectroscopy to study an electrode under potentiostatic control in an electrolyte medium. Fleischmann et al. [6] obtained Raman spectra of pyridine adsorbed on a silver electrode at various potentials in the 900-1050 cm^{-1} spectral region. [6] These results were of great interest since they showed that the highly specific method of Raman spectroscopy could be used to get molecular information for in situ studies at an

electrode surface. Other spectroscopic techniques used for this purpose such as infrared absorption and internal reflection at optically transparent electrodes or specular reflection and ellipsometry either lack sensitivity as in the first two examples or do not show molecular specificity as in the latter two examples.

Raman spectroscopy is particularly well suited for studying electrode surfaces in situ because of its vibrational specificity. It has the following advantages over infrared spectroscopy: the low frequency vibrations as well as higher ones are easily obtainable; water, the most frequently used electrochemical solvent, is a weak Raman scatterer; and salt windows are not required. Its main and potentially overwhelming disadvantage is that it is an inherently weak effect, and one would not normally expect to obtain a Raman spectrum of a monolayer of molecules adsorbed on a surface. For this reason, Fleischmann et al. [6] chose pyridine, with its relatively large Raman scattering cross section, as well as its sensitivity to environment, and a chemical pretreatment of the electrode designed to increase the surface roughness and therefore the surface density of Raman scatterers.

It was later pointed out by Albrecht and Creighton [1] and Jeanmaire and Van Duyne [7] that the intensity of the Raman spectrum of pyridine adsorbed on silver was anomalous. Fleischmann et al. [6] had repeatedly cycled their electrode

and thus increased the surface area by about ten. They assumed that the spectrum was observable due to increased coverage resulting from the roughening. Albrecht and Creighton [1] used a single cyclic voltage sweep which only increased the area by 10 to 20%. Calculations showed that the surface spectra were about 10^5 more intense than solution spectra since the scattered light is collected from 10^5 times fewer molecules on the surface. This intensity enhancement is the as yet unexplained phenomenon, which fortuitously enables the use of the Raman spectroscopic technique for studying adsorbed monolayers.

The work on SERS was then directed towards a better understanding of the following four features: 1) the kind of molecular and surface information obtainable, 2) the kinds of molecules, surfaces and environments it was applicable to, 3) the explanation of the phenomenon in both classical and quantum mechanical terms, and 4) new experimental applications.

There are several other techniques presently available for studying surfaces. Surfaces may be probed by low energy (less than 1000 eV) electrons which penetrate 1-2 nm, (or high energy electrons at a glancing angle to avoid deep penetration) photons, which penetrate 10-1000 nm or ions with less than 1000 eV energy which penetrate 1-2 nm. The output signal may be based on adsorption, emission or scattering. The combination of these probing methods and

output signals gives a wide selection of techniques for surface studies, each with different information about the surface.

Auger spectroscopy uses electrons of 2-3 keV to ionize inner electrons. Outer electrons fall into the vacancies leading to x-ray emission, or the energy may be given to another electron in the atom in the Auger effect. The Auger electrons are characteristic of the atom, giving qualitative and quantitative elemental analysis. Photoelectron spectroscopy (PES) using UV photons (also called ultraviolet photoelectron spectroscopy (UPS)), and X-ray photoelectronspectroscopy (XPS) also called electron spectroscopy for chemical analysis (ESCA) are similar to Auger spectroscopy but they use photons as probe beams to eject inner or valence electrons. These spectroscopies are more accurate than Auger and also provide valence electron structure determination. However they require ultra high vacuum and therefore are not useful for in situ studies.

Low energy electron diffraction (LEED) is often used in conjunction with Auger because the equipment is the same. LEED involves monoenergetic electrons of 1-500 eV impinging normal to a surface and the diffraction of elastically scattered electrons appear as spots on a phosphorescent screen. This shows the surface atoms' positions which may be different, but related to the bulk.

Secondary ion mass spectrometry (SIMS) uses an electron

beam of greater than 3 kV to form secondary ions which are detected by mass spectrometry. Scanning electron microscopy utilizes a deflected electron beam and detects secondary electrons. The resolution is about 10 nm, not on the molecular scale.

There are several other surface vibrational spectroscopies as well. Infrared transmission spectroscopy (ITS) is used for solid-gas systems of less than a monolayer. Infrared reflection specroscopy (IRRS) is used for solid-gas systems for studying a monolayer on a smooth, well-defined surface. High resolution electron energy loss spectroscopy (ELS) has good surface sensitivity but poor vibrational resolution and is used in a vacuum. Inelastic electron tunneling (IETS) provides good surface sensitivity but requires cryogenic conditions [8]. Internal reflection spectroscopy (IRS) or attenuated total reflectance (ATR) is similar to external reflection spectroscopy (ERS) but is light coming from a more dense to a less dense medium. It is due to the phenomenon, discovered by Newton, that the electromagnetic field associated with the light beam penetrates a certain distance beyond the reflecting interface. This yields optical spectra of adsorbed species and surface states [9]. Ellipsometry is also useful for determining thickness and the complex refractive index of an adsorbing film. This works through the depolarization of light and can measure thickness as low as 0.1 nm.

Surface Raman spectroscopy is applicable to solid-gas, solid-liquid and solid-solid systems. It can provide detailed information on the structure and orientation of surface molecules, the strength and nature of surface chemisorption, the structure of surface sites, catalytic reaction intermediates, and kinetics of surface chemical reactions.

Electrode pretreatment

Fleischmann et al. [6] electrochemically pretreated the electrode to roughen it to increase the surface coverage. They used a triangular wave cycling from -0.3 V to +0.2 V vs. a saturated calomel electrode (SCE) at the rate of 0.5 v/sec 450 times. This procedure yielded a 10^3 greater intensity than calculated. It was believed to have been due to some "hidden" resonance since pyridine absorbs only at wavelengths less than 280nm. Later Van Duyne et al. [2,7,10] reported a different electrode preparation procedure of mechanically polishing the electrode with 600 mesh Al_2O_3/H_2O slurry followed by a square wave potential starting initially from less than -0.22 to +0.20 V to -0.60 V vs. SCE. The electrode is anodized such that 25.0 millicoulombs/cm^2 are passed. This provides much less roughening but 30-100 times greater intensity than Fleischmann et al. observed. The SERS intensity increased with the amount of charge passed up to about 30 mC/cm^2, reached a plateau until about 50 mC/cm^2 and then decreased

with further charge transfer. When up to 50 mC/cm^2 are passed, 99.9% of the charge is recovered, leaving only 0.1% of the Ag as AgCl or Ag^+pyr. When the electrode is more positive than +0.08 V, Ag^o goes to Ag^+ which forms AgCl with the chloride electrolyte. When the electrode is more negative than -0.22 V, AgCl is reduced to Ag^o (and Cl^-). However, Dornhaus et al. [11] have shown that SERS can be observed before all the charge has been recovered. Fleischmann et al. originally observed a 10^3 enhancement over that which was calculated. [6] Van Duyne reports as much as 10^6 enhancement, [12] from his pretreatment, but also a 10^4 enhancement [7,10] with only the mechanical polish. Evans et al. [13] have shown that roughness on the scale of 100 nm, determined by SEM, which is produced after electrochemical pretreatment such as Van Duyne's allows maximum enhancement.

The initial reason for anodization was to increase the surface area and hence the number of molecules adsorbed on the electrode. However, although the surface area is indeed increased, the roughness achieved is not sufficient to explain the enhancement of 10^5-10^6. Another advantage of anodization is that the electrode is cleaned. Van Duyne et al. [7,10] performed AES analyses of the surfaces. Mechanical polish left S, C, Ca, and O impurities on the surface with C/Ag = 2.3 and O/Ag = 1.5 and O/Ag = 0.2. Mechanical polish and anodization with 30omC/cm^2 cleaned the surface even further yielding C/Ag = 1.1 and O/Ag = 0.1.

These AES results are confirmed by Evans et al. [13] with SIMS. Thus the anodization is seen to clean the surface, but the dramatic increase in intensity cannot be explained by cleanliness or roughness as a means for increasing surface coverage. The roughness produced must have some other effect to cause the enhancement, which will be discussed later. In conclusion, we see that anodization is not necessary, but roughening is. An optimally anodized electrode will, however, increase the intensity of the spectrum by a factor of 100 over the unanodized surface.

Roughness

Evans et al. [13] show with SEM that the amount of charge passed during the electrochemical pretreatment causes different scales of roughness in the form of nodular deposits. With 50 mC/cm^2 non-uniform nodules form with height and lateral spacing of 600 to 1,000 nm. With higher amounts of charge, 500mC/cm^2, the nodular size remains constant while the space between them decreases to 30 nm on the average. The intensity obtained from Raman scatterers is not reported, but from other results [7], 50 mC/cm^2 is in the range of maximum enhancement while 500 mC/cm^2 is well beyond that. They also claim that the surface area is increased by a factor of three to four. The reforming of the Ag surface during the oxidation reduction cycle serves to purify the surface and change the physical nature of the electrode surface. They believe the reformed surface is

consistent with the theories invoking resonant coupling to surface plasmon states since roughness is required for coupling of electromagnetic radiation to those states.

Rowe et al. [14] also studied the effect of surface roughness and found no Raman signal for a monolayer of pyridine for low index Ag (111) and (100) surfaces, for stepped Ag (100) surfaces or selectively etched Ag (100) with 2000-5000 nm facets. (For their experimental conditions this implies enhancement of less than 10^2. They did find enhancement on the order of 5 X 10^4 for surfaces having particles on the order of 100 nm separated by 150-300 nm. This surface was prepared using iodine vapor and 488.0 nm light, or with a single oxidation-reduction cycle in an electrochemical cell followed by Ar sputtering to remove impurities. They conclude that the theories must be modified to include the electromagnetic antenna-like enhancement of the small Ag particles.

Creighton, Blatchford and Albrecht [15] have reported intense Raman scattering by pyridine adsorbed on silver or gold aqueous sol particles of wavelength dimension. The intensity is strongly dependent on the excitation wavelength. A sharp resonance Raman maximum is observed at the wavelength of the Mie extinction maximum of the metal particles. They propose that the resonance Raman phenomenon is the Raman component of resonant Mie scattering and the polarizability of the metal particles is modulated by the

vibrations of the adsorbed molecules. This would comfirm that surface plasmons are involved in SERS.

Silver Surface

The enhancement is observed with many types of Ag by many different groups. Many groups have observed the effect on polycrystalline wire or foil. Pettinger et al. [16-18] have done work on Ag (100) and Ag (111) single crystals and Ag (111) epitaxial thin film electrodes (TFE) formed by high vacuum vapor deposition on mica substrates. The intensity on the TFE is down by only a factor of 2. In the single crystal studies, the intensity was comparable to polycrystalline experiments, but the relative intensity as well as frequencies are sensitive to the crystal orientation. They interpret the polycrystalline results as being a superposition of the Raman spectra for pyridine at surface sites with different orientations. (The results of Pettinger et al. are obtained on reformed Ag surfaces which may or may not have the same orientation as the initial bulk metal.)

Solution

The enhancement also seems to be somewhat dependent upon the concentration of the Raman scatterer and the electrolyte. Barradas and Conway [19] have shown, using UV-visible absorption, that the bulk concentration of pyridine required to achieve saturation in the isotherm is

about 1.5 X 10^3 smaller than the 50 mM bulk concentration of pyridine [7] required to achieve saturation in the Raman detected isotherm. The need for such a large bulk concentration may indicate a multilayer or orientation requirement. High concentration may be required to make the molecules sit perpendicularly to the Ag surface. Jeanmaire and Van Duyne [7] made a study of the bulk chloride concentration on enhancement and found a ratio of two Cl^- to one pyridine gave optimal enhancement. However, Erdheim [20] has shown that the maximum intensity for differnt lines varies with anion as well as anion concentration and potential. This is clearly a complex interdependence. Jeanmaire and Van Duyne [7] have shown that the cation has no effect and this is confirmed by Evans et al. [13]. The only other solvent which seems to allow the effect is a methanol water mixture which aids the solvation of some molecules not soluble in water alone. The degree of solubility does not seem to affect the SERS. Jenamaire and Van Duyne [7] studied the pH dependence and found that as the pH is reduced from 5 to 3 the intensity goes to zero and remains zero as the pH is further reduced. For pH 13-5 the intensity is constant. They attribute the loss of intensity to the formation of pyridinium ion. Regis and Corset have recently reported spectra obtained at low pH, and in fact attribute the spectra observed to adsorbed pyridinium. [21]

Electrode potential

The electrode potential has a small but definite effect on the SERS. Fleischmann et al., [6] Jeanmaire and Van Duyne, [7,10] and Pettinger and Wenning, [18] have all shown that the Raman intensity, number of lines observed and the vibrational frequency of the lines are all functions of the electrode potential. ΔG^{o}_{Ads} is a strong function of the potential which exists in the compact double layer which is 1-5 X 10^{6} volt cm^{-1}. Jeanmaire and Van Duyne studied the potential dependence of six of the intense peaks of pyridine by scanning the potential vs. time from 0.0 V to -1.0 V at 1.0 V/sec. This produced a factor of 4-5 change in the intensity, although the maximum intensity was not at the same potential for each line. These curves were, however, very similar to Γ vs. $E-E_z$ curves (where is surface concentration ($moles/cm^2$), E = electrode potential, E_z = potential of zero charge (pzc)) for class II adsorbates (neutral organic molecules). The curves, however, are slightly asymmetric which Jeanmaire and Van Duyne [7] attribute to variable Cl^- or H_2O absorption. When the electrode is positive vs. pzc, the Cl^- concentration of the electrode is relatively high and therefore more pyridine is induced to adsorb. When the electrode is negative relative to the pzc the Cl^- concentration is low and the pyridine must compete with water. (However, one might expect to see SERS for water at more negative potentials as there are some indications that any molecule near the surface should show

SERS. This will be discussed later.) Jeanmaire and Van Duyne [7] were able to show that the signal tracks the charging potential very well. They changed the potential from -0.1 V to -0.6 V with a duration of 0.010 sec at -0.6 V. The rise and fall of the intensity was not perfectly sharp due to a finite double layer charging time of about 0.1 m sec. At bulk pyridine concentrations of about 50 mM, longer rise and fall times are observed. However, these results do show that SERS can be used to study surface kinetic phenomena. The potential modulation of the intensity as well as the small shifts may be due to varying orientation, but clearly, since the potential has an effect to maximally 10 nm from the surface we are seeing surface phenomena.

Venkatesan et al. [22] found that the 240 cm^{-1} band shifts to lower potentials with decreasing electrode potential. The square of the frequency was found to be directly proportional to the electrode potential, and the intensity and line widths also a strong function of potential. This is explained by the effect of the electric field in the double layer on the dipole moment of the adsorbed molecule. The force constant of the Ag-N vibration was shown to depend on three contributions: a) the force constant in absence of the field, b) the imaging of the molecule in the electrode and c) the discreteness of charge of the specifically adsorbed anions, which is a function of the electrode potential and gives rise to the observed shift

of the Raman band.

Laser power

Van Duyne [12] reports that the intensity for pyridine on Ag is a linear function of laser power for the 514.5 nm laser line with a power of 0-120 mW, and similar results for other continuous wave (CW) excitation wavelengths. He reports similar results for a flashlamp pumped, pulsed dye laser operating at 10 mj per pulse (10 kW peak power) and 5 pps (600.0 nm).

Long exposures to the laser may have thermal, photochemical or photoelectrochemical effects on SERS. Dornhaus et al. [11] note variations in the peak intensities for pyrazine/Ag at -0.4 V in a four hour period. Van Duyne [12] reports no changes in the pyridine/Ag SERS over a period of 1-5 hours of exposure to 514.5 nm at 100 mW for potentials more negative than -0.6 V. He describes the reduction of the 1037 cm^{-1} line and the growth of the 1006 cm^{-1} line which occurs with time at potentials more positive than -0.2 V as laser damage. There appears to be some interaction of the potential, laser exposure, and compound which causes the SERS to change somewhat, but this has yet to be explained.

Laser frequency

The dependence of intensity on exciting frequency, ω_L, is of great interest because of the clues this dependence

might provide for the explanation of the enhancement. Normal Raman spectra show an ω_L^4 dependence while resonant Raman spectra show a complex frequency dependence. Generally, departures from the ω_L^4 dependence indicate the existence of pre-resonance or rigorous resonance Raman spectroscopy. Resonance Raman spectroscopy shows a 10^6 enhancement over normal Raman spectroscopy, so it was natural to suppose that the adsorption of the pyridine on the silver had created some sort of resonance condition.

The reproducibility of ω_L dependence is rather poor from group to group, which is remarkable in view of the good reproducibility of SERS in terms of relative intensity, line frequency and even potential dependence. This may be due to the fact that most groups do not use internal standards and therefore do not measure the absolute intensity and because absolute intensity seems to be highly dependent on electrode pretreatment.

The early studies [7,10] of the excitation profile dependence were designed to show only that the 514.5 nm excitation was not unique for SERS, that there was no wavelength at which SERS suddenly appeared and no order of magnitude changes in intensity. Indeed it was found that over the range 457.9 to 650.0 nm there was no strong departure from the ω_L^4 scattering law. [7,10] (No internal standard was used.) However, variations in the relative intensities of some lines, including 1037 cm^{-1} and 1006 cm^{-1}

were noted. This relative intensity variation is not noted for neat or aqueous pyridine in bulk media.

Creighton et al. [23] studied the excitation profile for the 1008, 1026 and 1036 cm^{-1} line of pyridine/Ag for an exciting wavelength of 457.9 to 632.8 nm using the $NaClO_4$ and water bands as internal NRS intensity standards. The intensity of these SERS lines showed a factor of 20 increase as ω_L decreased suggesting that SERS does not obey the ω_L^4 scattering law.

Pettinger, Wenning and Kolb [17] independently verified this work by Creighton et al. In addition, they measured the differential reflectance spectrum of their single crystal and found an electronic absorption band that peaks around 750 nm. This adsorption feature was produced only after anodization. The excitation profile and the absorption feature led them to assign the SERS scattering mechanism as a resonance Raman effect. They did not rule out, however that they were observing a resonance Raman effect superimposed on an underlying SERS mechanism.

Allen et al. [24] (using an internal standard of pyridine-d-5 normal Raman spectrum which will be explained in greater detail later) found the same general trend for the 1037 and 1008 cm^{-1} bands but found the 1215 cm^{-1} band to follow rigorous ω_L^4 dependence. They used a different potential than the Creighton and Pettinger groups, therefore they studied ω_L^4 deviations with respect to laser exposure

time and potential. In general, the deviations were more pronounced the more positive the potential, the longer the exposure, and if more than 50 mC/cm^{-1} were passed during anodization.

In conclusion, we do not see the typical laser frequency dependence of either resonance or normal Raman spectroscopy. The laser frequency dependence varies with anodization, potential and exposure time, just as the other Raman observables vary.

Incident angle

Pettinger, Tadjeddine and Kolb [25] have studied the effect of the incident laser angle on Ag samples and found the maximum enhancenent to be at 50 degrees. Wenning, Pettinger and Wetzel [26] found the angle of maximum intensity for copper to be $61\pm10^{\circ}$ and for gold $59 \pm 10^{\circ}$. This strong angular dependence was suggested as proof of coupling into surface plasmons, as an explanation for enhancement. This will be discussed in greater detail later.

Surface spectroscopy

The high bulk concentrations of pyridine required over that necessary to achieve full surface coverage [19], as well as the interpretation by Albrecht et al. [27] that the delayed intensity response to potential changes is due to capillary adsorption both call to question whether SERS is

actually a surface spectroscopy. Several groups have investigated the surface nature of SERS, ranging from experiments to show that only molecules near the surface are enhanced, to proving there is only a monolayer.

Van Duyne [12] applied a two-channel, potential dependent form of SERS, surface enhanced Raman potential difference spectroscopy, SERPDS. Two spectra, one at E_1 = -0.2 V and one at E_2 = -0.8 V are taken simultaneously by putting a square wave potential with voltage limits E_1 and E_2 at a frequency of 1-10 Hz on the electrode. The spectra are fed to two gated channels and fed to a computer which calculates the difference spectrum. The resulting non-zero spectrum is due to only the Raman scatterers which exist within the double layer. For 0.1 M KCl the double layer is less than 10 nm, but most of the potential drop occurs within the compact double layer which is less than 1 nm. Also both the frequency and linewidth were shown to be potential dependent for the 1006 and 1037 cm^{-1} lines.

Smardzewski et al. [28] studied pyridine and pyridine-d-5 on argon ion cleaned electrodes at 77 K in UHV. By separately investigating spectra of monolayers of pyridine, pyridine-d-5, and mixtures of the two, they found that it is the species immediately adjacent to the metal surface whose Raman spectrum is appreciably enhanced.

Murray [29] has worked on experiments involving a CaF spacer between the Ag surface and Raman scatterer. She

finds some enhancement for molecules at distances up to 5 nm from the surface. This seems to be in contradiction to the previous group's work which shows no enhancement for layers not immediately adjacent to the silver surface. The discrepancy is explained by Murray as difficulty in determining the precise coverage.

Bergman et al. [30] performed radioisotope measurements to determine surface coverage of cyanide on Ag. They determined that the SERS peak (CN stretch at 2144 cm^{-1}) is indeed from a monolayer of cyanide (about $10^{15}/cm^{-1}$). Their experiments were performed in air.

Erdheim et al. made a careful vibrational analysis of pyrazine SERS. Pyrazine has D_{2h} symmetry as a free molecule which separates Raman active and IR active vibrationl modes into distinct groups. This distinction no longer holds for the SERS where all the vibrations have become Raman allowed. This is due to a lowering of the symmetry to C_{2v}, strong indication of some sort of surface complex.

Enhancement

In order to determine the absolute enhancement, the number of molecules on the surface has to be measured. A very good way to do this is via chronocoulometry. This is a measurement of charge vs. time for an electroactive species. A plot of this charge vs. $t^{1/2}$ will be linear and the intercept proportional to the surface coverage of the

electroactive species. Then enhancement of the molecule on the surface can be compared to the solution. However, it is difficult to compare an intensity of an electroactive species at the potential of reduction, because of the chemical changes that are going on. Van Duyne [12] did exactly such a chronocoulometric experiment on 4-acetylpyridine and used the value he obtained for surface coverage of 1.95×10^{14} molecules/cm^2 as the value for pyridine. This assumption that the surface coverage for pyridine is the same as for 4-acetylpyridine, would not cause errors on the scale of several orders of magnitude. To prevent problems with instrumental variations, he has devised a cell in which he can simultaneously take normal Raman spectra of one solution and SERS of another solution, with well defined volumes and areas. He does this for pyridine-d-5 and pyridine where he could look at strong, non-overlapping vibrations in each molecule and compare the intensities. He used the 966 cm^{-1} pyr-d-5 band and the SERS 1008 cm^{-1} band of pyridine. He calculated the enhancement factor of 1.3×10^6. (using his numbers and equation, I calculate 9.2×10^6.)

Continuum

There is a strong background continuum which has three regions: below 200 cm^{-1}, rising to 1600 cm^{-1} and out to 4000 cm^{-1}. The region around 1600 cm^{-1} was originally thought to be due to adsorbed carbonate [31]. Mahoney et al. [32]

assign this to CO_2 (at pH 5.5) and CO_3^{2-} (at pH 11) which is electroreduced to an unstable silver surface-formate complex which in turn spontaneously decomposes to graphitic carbon surface layers. Heritage et al. [33], through picosecond Raman gain experiments, have shown that the region of the continuum near 2000 cm^{-1} is not a Raman effect, but due to luminescence. The low frequency region may be due to molecular librations. Pettinger [34] describes the continuum as a superposition of numerous extremely weak SERS lines attributed to complexes of metal-adatom pyridine and halide ions.

Raman Observables

Pyridine was the first molecule selected to study with Raman spectroscopy on an electrode surface because its vibrations are sensitive to environment. This was a fortuitous choice, and many studies were made on adsorbed pyridine although a complete study of Raman observables, intensity, frequency, depolarization ratios and line shapes has not been published to date. However, the results presented so far are quite interesting. Much of this work has been done by Jeanmaire and Van Duyne [7]. The shifts of all the modes are only 2-20 cm^{-1}, which is small, indicating the electronic structure of pyridine is not dramatically perturbed by the 1-5 x 10^6 V cm^{-1} electric field in the compact double layer. The 216 cm^{-1} band is attributed to Ag-N because it has no solution counterpart and is observed

at potentials as negative as -1.1 V, at which Cl is desorbed. The 239 cm^{-1} band is observed only at potentials more positive than -0.4 V and is therefore attributed to AgCl. At least one band from every symmetry type can be observed. The depolarization ratios for SERS are all 0.6 to 0.7 while in NRS they are 0.01-0.03. This may be partially explained by the assumption that pyridine is bonded axially through the nitrogen and is undergoing two-dimensional rotational averaging of the scattering tensor. The line shapes are broader in SERS than in solution of neat spectra. The latter two have Lorentzian line shapes but SERS does not, which is probably due to the surface environment. Birke and Lombardi have done a detailed analysis of the line shape of Ag-N for several molecules [35] and have concluded that it is exceedingly broad due to different surface environments. Pettinger and Wenning report different line widths for Ag (100) and Ag (111) [16]. The effect is not limited to pyridine. Other molecules that show enhancement are piperidine, aniline, N,N-dimethylaniline, benzylamine, N-methylimidizole, sulfanilic acid, 2,4,6-trimethylpyridine, 2-, 3- and 4-cyanopyridines, 2,4-dicyanopyridine, 4-t-butyl-pyridine, pyridine-d-5, 4-acetylpyridine, N,N-dimethylcyanamide, and pyrazine [36]. Ammonia, however, does not show enhancement [37].

II. THEORY

Many theories to explain the SER effect have been presented, which vary from descriptive to detailed calculations. In order to satisfactorily explain the effect, a theory must not only be able to explain all the data, but must also be a quantum mechanical self-consistent mechanism. The fact that many of the theories are only descriptive and that many of them are similar makes them not mutually exclusive. It is not so much that several mechanisms may be responsible for the effect, which may be true, but that the mechanism may be described in several different ways. Some of the more outstanding data which the theory must explain follows: 1)the effect is greater on Ag, definitely appears on Cu and Au with red excitation, and possibly on Pt, 2) Deviation from $(\hbar\omega)^4$ dependence, 3) the existence of a background continuum, 4) molecules which show resonant Raman scattering show an additional enhancement when adsorbed, 5) the enhancement is maximal on surfaces with at least 100 nm roughness (although this has yet to be unambiguously determined), 6) some molecules do not seem to show SERS although a large variety do, 7) overtones are weak or non-existent, and 8) SERS is always depolarized. A complete theory of inelastic light scattering from a molecule adsorbed on an electrode must incorporate specific adsorption of the molecule, electron wavefunctions of the molecule and surface localized electron states of the metal and charge rearrangement in the metal

and molecule. The molecule-metal interactions can be separated into field interaction, involving coulomb interaction, and electronic interactions, involving hybridization, charge transfer or charge sharing. Implications for other processes such as photon absorption, luminescence and photocurrents must also be considered.

The enhancement is the differential cross section per molecule. This may be due to a modification of the molecule itself, a coupled molecule-metal scatterer or collective behavior such as coherent scattering. The Raman cross section is proportional to:

$$d\sigma = (\hbar\omega_s)^4 |\bar{\alpha}|^2 \qquad (1)$$

where $\hbar\omega_s$ is the photon energy of the scattered radiation and $\bar{\alpha}$ is a component of the Raman scattering tensor. $\bar{\alpha}$ describes the normal coordinate derivative of the molecular polarizability α:

$$\bar{\alpha} = \frac{\partial \alpha}{\partial Q} dQ \qquad (2)$$

In the microscopic analysis is expressed as a sum over virtual intermediate states:

$$\bar{\alpha} = \sum_j \frac{\langle f|H|j\rangle\langle j|H|i\rangle}{(\epsilon_j - \epsilon_i) - \hbar\omega - 2\Gamma_i} \qquad (3)$$

where $|i\rangle$, $|j\rangle$, and $|f\rangle$ are electronic vibronic molecular initial, intermediate and final states respectively, $\hbar\omega$ is the incident photon energy. H represents the transition dipole operator. The lifetime of the intermediate state, $2\Gamma_i$, is included to allow for the possibility of correspondence to a real molecular state, the resonant Raman

condition. The microscopic approach must then account for conditions where $\omega = \epsilon_j - \epsilon_i$ or enhanced matrix elements in the numerator. Since the enhancement is proportional to $|\bar{\alpha}|^2$, $\bar{\alpha}$ must be enhanced by approximately 10^3 to account for the nearly 10^6 enhancement.

The theories fall into loose groupings since they are not exclusive. They are image field, modulated reflectance, adsorption induced resonance, geometry defined resonance and microscopic theories.

i. Image field theories:

These theories are put forth by King, Van Duyne and Schatz [38], Efrima and Metiu [39], and Eesley and Smith [40]. These three theories discuss the total optical field felt by the adsorbed molecule and use a point dipole approximation for the charge distribution of the molecule. Although exactly how the field interacts with the dipole moment (μ) is treated differently in each theory, it is essentially the mechanism:

$$\mu = \alpha_0 (E_0 + E_d) \qquad (4)$$

where α_0 is the polarizability of the free molecule, E_0 is the incident field, and E_d is the field at the molecule which is caused by the image of the dipole in the adjacent metal. Since the system responds as a whole, an effective polarizability can be defined as:

$$\alpha_{eff} = \frac{\mu}{E_0} = \frac{\alpha_0}{(1 - \alpha_0 E_d/\mu)} \qquad (5)$$

As $\frac{\alpha E_d}{\mu} \rightarrow 1$ the effective polarizability is greatly enhanced.

E_d is the result of a self-image and can be written, as in King, Van Duyne and Schatz as:

$$E_d = \mu\left(\frac{\epsilon_m - \epsilon_A}{\epsilon_m + \epsilon_A}\right)\frac{1}{4R^3} \qquad (6)$$

where ϵ_m and ϵ_A are the metal's and ambient medium's complex dielectric functions respectively and R is the effective molecule-surface separation. Changes in R of only a few thousandths of a nm can have dramatic effects on the enhancement of the scattering. Physisorption is implied since any perturbation of the molecule is neglected as seen in equation (4), the linear approximation for α.

Efrima and Metiu, in their image field theory, use the Green function technique to solve the scattered distribution problem. They also include additional contributions to the enhancement from the character of incident and scattered radiation fields obtained from Fresnel equations in the vicinity of the surface.

The theory of Eesley and Smith includes the total field contributions from adjacent molecules and their images. They also use an interaction Hamiltonian formalism which contributes to the intensity as follows:

$$I \sim |H_{int}|^2, \quad H_{int} = \frac{\partial(\alpha E)^2}{\partial Q} dQ \qquad (7)$$

This can be written as $\left(\frac{\partial E}{\partial z}\right)\left(\frac{\partial z}{\partial Q}\right)$ where z is the coordinate $\perp$ to the surface, Q is the molecular coordinate of the mode in question, and E is the local field. This term can be non-zero even when $\frac{\partial \alpha}{\partial Q} = 0$ which may lead to the background continuum.

The image field models predict that infra-red absorption will also be enhanced. Some excitation energy dependence is derived from dynamic screening characteristics of the metal which enter through ϵ_m. The dynamic screening ability is better for Ag than Au or Cu but Hg is predicted to be nearly as effective as Ag in the visible. Two criticisms with the image field theories are that they extend a linear response to a non-linear realm and that the metal surface is considered as a plane unperturbed by the adsorbate. Hilton and Oxtaby [41] performed model calculations to show that the enhancement calculated for the image dipole models results from the use of an asymtotic theory at unphysically short distances.

ii. Modulated reflectance theories:

This next group of theories includes the ideas of Otto [42] and McCall and Platzman [43] which deal with the modulated reflectivity model. They derive the enhancement from the interaction of photons and the electrons in the metal. In Otto's theory, the vibrating molecule modulates the surface charge density of the metal through the electric field between the molecule and metal. He uses electroreflectance theory to specify the interaction between the photons and the modulated electrons. Otto also uses electron Umklapp processes to increase the enhancement to 10^6, and also explains the continuum background, and points out that the Umklapp processes are larger with surface

roughening. McCall and Platzman postulate that the surface charge density is modulated by the vibration of the electronic cloud of the chemical bond which follows the vibration of the atom chemically bonded to the surface. This modulates the susceptibility of the molecule-metal complex which produces the Raman enhancement.

These two models differ from each other in their excitation energy dependence because of the way the oscillating molecule is coupled to the surface electron density oscillation. McCall and Platzman predict there should be no excitation energy dependence, not even $(\hbar\omega)^4$. In Otto's derivation, the intensity depends on $(\hbar\omega)^2 f^2$ where f is the change in metallic reflectivity with the applied electric field, which for free electron metals is $(\hbar\omega)^2$. For visible incident light, Cu, Ag, and Au have approximately equal electro-reflectance intensities which increase with excitation energy. For these theories, as well as the image field theories, molecules which are resonant in the free condition will display an additional enhancement in the adsorbed condition. In the McCall-Platzman theory the chemical bond is very important and strong overlap is important. In Otto's theory, long-range forces are sufficient and only physisorption is required.

iii. Adsorption induced resonance theories:

This next group of theories is based on resonant Raman

scattering brought on by adsorption induced perturbation of the electronic states of the molecule. Included in this group are the prediction by Philpott [44], actually made before the SER effect was discovered, the second mechanism by Efrima and Metiu [45], a proposition by Pettinger, Wenning and Kolb [17], a calculation by King and Schatz [46], and a model of Regis and Corset [21].

Philpott's theory is the quantum field limit and Efrima and Metiu's theory is the classical field limit of the same idea. Molecular and electronic transitions for molecules adsorbed onto metal surfaces display shorter lifetimes and lower energies [47]. The smaller lifetimes give rise to a broadening of the transitions. These effects are caused by Coulomb interaction between the molecule and the metal which shifts and broadens the energies of the individual electronic states. This is a long range effect. The electronic levels of the adsorbates become effectively broad bands between which photoexcitation can occur. This amounts to a renormalization of the molecule states to include, by virtual photon transfer, a coupling to dissipative channels in the metal. Topographical surface roughness is not required to effect this coupling. Radiative electromagnetic modes (plane waves) and non-radiative modes (surface plasmons) can be coupled with an entity on the surface which breaks the translational symmetry in the surface plane to allow the conservation of momentum and energy at the same time. A rough surface satisfies this symmetry-breaking

condition but the radiation from the molecules contains the entire spectrum of Fourier components in momentum space and can couple to surface plasmons without surface roughness.

The biggest problem with these two theories is that at small distances applicable to the absorption situation, the formalism is incomplete. Both the quantum and classical approach to the problem of molecular luminescence are successful since they bring the molecule no closer than about 2.5 nm. When this distance is made smaller the problem must be solved self-consistently, with a determination of the combined states of the molecule-metal system, allowing for charge transfer as well as Coulomb interaction.

Regis and Corset propose that the enhancement is due to resonant Raman scattering of pyridinium radical cations and pyridinyl radical anions formed from Ag-pyr-Cl complexes, as well as pyr-HCl, Ag°pyr complexes, and Cl_2^- species. However this might explain only the results for electrodes and not the vacuum or ambient air SERS. The existence of such radical ions has not been demonstrated but only hypothesized. This could be easily checked by ESR studies which can now be made with electrodes in situ.

iv. Geometrically defined surface resonance theories:

This group of theories contains the resonance electron absorption model of Moskovits [48] (which was presented as a

theoretical report), part of a theoretical discussion by Hexter and Albrecht [49], the interpretation of Creighton, Blatchford, and Albrecht [50] which was used to explain some of their data on sols, and a theory by Gersten and Nitzan [51]. The concept involved in all of these theories involves resonant absorption by collective modes in the free electron gas in the metal which is coupled to the vibrational modes of molecules adsorbed on the surface. The mechanism is similar to that involved in organometallic compounds such as porphorins. A porphorin with a metal will show resonant Raman behavior throughout the entire molecule--the mechanism of excitation transfer occuring because of delocalization of electrons. In Moskovits and Creighton, Blatchford and Albrecht and Gersten and Nitzan theories the absorption occurs in particles much smaller than the optical wavelength and with restricted geometry. The first is concerned with a two dimensional colloid while the second is concerned with a metal colloidal suspension, and the third is concerned with metal spheroids. (The calculation of normal modes of electron gas for restricted geometries has been done by Mie [52] for isolated particles and by Maxwell-Garnett [53] for more closely packed particles.) The plasma resonance condition can only be sustained in metals without excessive damping avenues such as interband transitions. The noble metals, especially silver, fill this condition and are known to easily form colloidal suspensions which produce optical electronic

resonances in the visible region of the spectrum. Neither of the first two theories addresses the crucial question of how the coupling between the photons and electron gas finally couples with the vibrational modes of the adsorbed molecules to give the resonant Raman scattering. Hexter and Albrecht suggested extending these ideas to other geometries such as planar metals.

The Moskovits and Creighton, Blatchford and Albrecht theories both predict that since the geometry affects the energetic position of the resonance, the $\hbar\omega$ dependence should vary with the sample. Hexter and Albrecht predict the scattering should be independent of $\hbar\omega$ because of their assumption that the intensity is proportional to coupling between the surface plasmons and the molecule. At low $\hbar\omega$, the density of the surface plasmon modes varies as ω^{0} whereas the interaction matrix, assumed proportional to the metal extinction coefficient, varies as ω^{-1}. Coupling between the photon field and surface plasmon is not discussed by Hexter and Albrecht.

Gersten's second theory [51] considers the surface roughnes as spheroids and calculates enhancement while varing the aspect ratios of the spheroids. The enhancement can arise from three sources: the electric field near a sharp object is intensified, the image of a dipole induced in a spheroid is larger, and coupling to surface plasmons will all cause enhancement. These account for 10^5, 10 and

10^5 enhancement factors respectively, which gives quite a large predicted enhancement. (The 10^6 enhancement calculated is always a minimum.) However, the calculations cannot be made for small scale roughness on the order of adatoms, although the calculations for particles of 10 X 50 nm size show good correlation to enhancement observed.

v. Electron-hole excitation theories:

This last group of theories contains the most microscopic theories with explicit statements and/or calculations of the detailed excitation-relaxation processes involving the electron states in the molecule and metal and the vibronic states in the molecule. The group contains the theories by Gersten, Birke and Lombardi [54], Burstein, Chen, Chen, Lundquist and Tosatti [55], and by Fuchs [56].

Burstein et al. describe four mechanisms which involve electron-hole pairs in the metal, but provide no calculations to support these ideas. They emphasize the role of surface roughness in producing e-h pair excitations through coupling to electromagnetic radiation. Two of the mechanisms are field or Coulomb interaction. The e-h excitations in the metal surface are transferred to electronic excitations in the molecule creating a molecular vibration in the interim. In the second mechanism the e-h pairs form e-h polarons which become real vibrations. The other two mechanisms involve electronic interactions. The electron and hole scatter inelastically from the molecule,

as in inelastic tunneling, but return to the electrode of origin. In the last mechanism, the e-h is excited to a virtual bound state of the molecule and de-excitation leaves the molecule in a vibrationg state. All these theories require surface roughness to provide parallel momentum which creates the e-h pairs.

In the Gersten, Birke, Lombardi mechanism the upper level (ϵ_b) of the molecule is broadened through interaction with the metal electronic states (through weak chemisorption) which allows electrons to be photo-injected into the metal provided $\hbar\omega + \epsilon_a$ (the ground state level) $\geq$ E (the Fermi level). This results in a shift of the Fermi level. Recombination produces a broad luminescence band. (This would explain the continuum background scattering.) If the interfacial potential difference is changed far enough by the potential applied on the electrode the enhancement would be cut off. ($\hbar\omega + \epsilon_a$ would no longer be $\geq$ E .) The theory predicts a small photocurrent due to the photo injection process which is observed for electrode SERS but would be impossible in other SERS. Experiments involving two excitation lasers simultaneously have shown a spectrum which is the sum of two, one associated with each excitation energy. This disproves the induced shifting of E since this could only be satisfied by one of the exciting lines.

The Fuchs theory involves e-h excitation in a treatment of the surface optical properties by non-local

electromagnetic theory. The theory separates interactions between the incident photon and the electrons of the metal to create the virtual intermediate state, between the electrons and the molecule in the intermediate state to produce a vibrational transition, and between the virtual excitation of the electrons and the scattered photon. The perpendicular fields, when described using non-local formalism, induce a surface charge and high momentum oscillations which are the e-h pairs. Two mechanisms could provide coupling to the molecular vibrations: e-h scattering by the Coulomb field of the molecule dipole and resonant scattering by a molecular virtual level which lies above the Fermi energy of the metal. A conceptual difficulty with this theory is the boundary conditions for the non-local fields and the non-local optics become very complicated with surface roughness. The exact excitation energy dependence is dependent on many parts of the theory, the creation of e-h pairs, excitation to the virtual bound state, and scattering interaction mechanism.

Discussion

The image field models depend critically on proximity and recent work [57] has shown that not only proximity but the character of the bond is important to the enhancement. Molecules which show resonant Raman scattering show an additional enhancement when adsorbed [7]. This implies that the resonance mechanism is still acting in the adsorbed

molecule, a condition which would seem to preclude an additional adsorption induced resonance. However, the conventional resonance Raman could arise from molecules not specifically adsorbed on the surface. The absence of overtones also supports the non-resonance models. Lifetime measurements on the picosecond time scale would differentiate between resonant and non-resonant conditions.

The modulated reflectance models do not correspond to the measured $\hbar\omega$ dependence. McCall and Platzman predict no change in intensity with $\hbar\omega$ while Otto predicts a rapidly increasing intensity with $\hbar\omega$. Both theories predict Au should show a larger enhancement than Ag at 2.5 eV, which is not observed.

The induced resonance models of Philpott and Efrima and Metiu predict a complicated $\hbar\omega$ dependence which is observed. They also predict some enhancement for molecules not immediately adjacent to the surface which has been demonstrated [58]. Both the image field models and the induced resonance models predict proximity alone should be enough to give enhancement which has been demonstrated not to be true [57].

The geometrically defined resonance theories correspond to nearly all the experimental evidence. The only experiments against this are those of Pettinger et al. [17] which show a lack of optical detection of surface plasmons on Ag under conditions which showed SERS, and the observance

of SERS from a smooth surface.

In suppport of the Pettinger et al. and Regis and Corset theories, Ag-pyr complexes are found during the anodization cycle [7,17], however that cycle is not necessary to show the effect. Also Ag-pyr complexes would not explain the non-electrochemical observances of SERS. Large shifts in the vibrational modes would be expected for pyridine complexes from those of neat or aqueous pyridine, which are not observed [49].

The variety of theories presented to explain the extensive data that seems to defy classical Raman interpretation will definitely lead to a truer explanation of the SER phenomenon. As yet, one theory is not sufficient nor are the domains of the theories exclusive; the combination of models leads to a better understanding of the mechanisms involved, if not yet on the quantum mechanical scale, at least on a macroscopic scale.

III. EXPERIMENTAL

Raman spectra were obtained with a Coherent Radiation 52B argon ion laser in conjunction with a SPEX 1401 double monochromator; slit widths were set to give an effective bandpass of 2.2 cm^{-1}. Signals detected by the ITT FW-130 photomultiplier tube were fed to a Harshaw NA12 DDL amplifier and NC-11 analyzer discriminator for photon counting.

The solution Raman spectra were obtained with a SPEX liquid cell model 1436. The electrochemical cell, electrodes and scattering geometry used for the measurements are shown in Figure 1. The reference electrode is a saturated calomel electrode (SCE), the counter electrode is a platinum wire, and the electrode at which spectra were taken is polycrystalline Ag. The silver electrode is angled at 45 degrees so that the laser light which comes up through the bottom of the cell is scattered at 90 degrees into the monochromator. There are openings for nitrogen bubbling for deoxygenation of the solutions. The total capacity is about 25 milliliters. Electrode potentials on the Ag electrode were controlled with a Princeton Applied Research (PAR) Model 173 potentiostat together with a PAR model 175 universal programmer. All potentials are quoted against that of the SCE.

All solutions were prepared using distilled deionized water. Reagent grade KCl from Fisher Scientific was used as

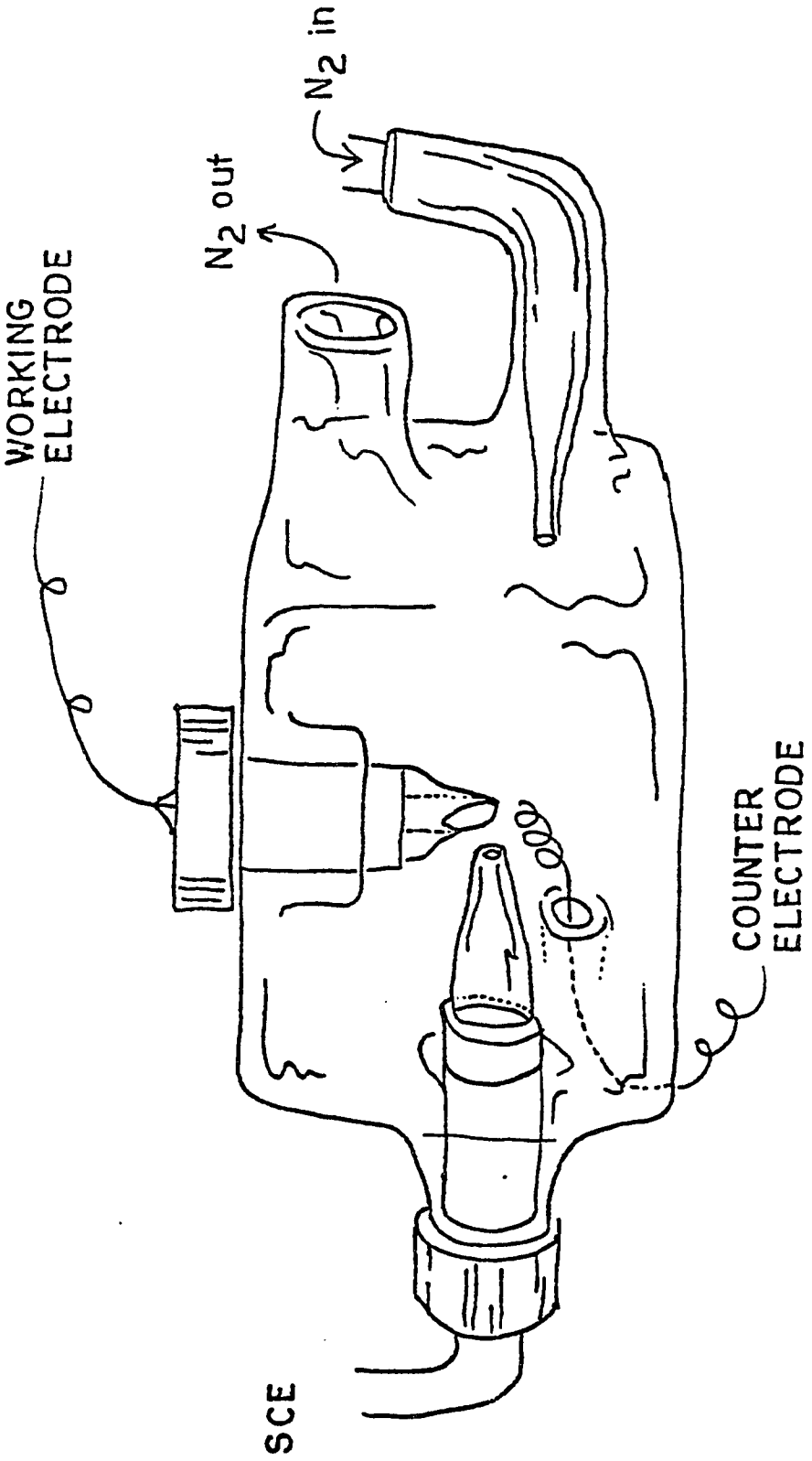

Figure 1. The electrochemical cell.

the supporting electrolyte.

The 2-methylpyridine (2-picoline), 3-methylpyridine (3-picoline), and 4-methylpyridine (4-picoline) were obtained from Aldrich Chemical Company in 98, 99, and 98% purity respectively. (The most likely impurities in the methylpyridines are the other isomers. Since the surface spectra are enhanced, small impurities could be important, but are not, since even the strongest lines in one methylpyridine are not observed in the other spectra, so further purification was deemed unnecessary.) The concentrations for the surface SERS were all 0.1 M in methylpyridine and 0.2 M KCl. The 2- and 4-methylpyridine concentrations for the NSRS were 1.0 M in 0.1 M KCl. The 3-methylpyridine concentration was 1.0 M in 0.2 M KCl. The electrochemical pretreatment procedure involved holding the Ag electrode at -0.6 v, then applying a square wave potential to +0.2 V. The potential was held at the positive value for 1 s then returned to - 0.6 V for the duration of the Raman experiment. All spectra were taken with the 514.5 nm line of the argon laser.

The 2,6-lutidine was obtained from Sigma Chemical Company and fractionally distilled before using. The concentrations for the SERS wer 0.05 M in 2,6-lutidine and 0.1 M KCl. The concentrations for the normal solution Raman spectra were 2 M in 2,6-lutidine and 0.1 M KCl. All spectra were taken with the 488.0 nm line of the Argon laser, except

for the regions of 350, 560, and 150 cm^{-1} which were also scanned with the 514.5 nm line because of plasma line interference with the 488.0 nm line. The electrochemical pretreatment proceedure involved holding the Ag elecrode at -0.6 v then applying a square wave pulse which stepped the elecrode potential to +0.2 V for 2 seconds then returned to -0.6 V. The pretreatment was carried out with only the KCl in the cell, then the 2,6-lutidine was added and the electrode was reanodized in the same manner. The spectra taken at potentials ther than -0.6 V were also stepped to +0.2 V for 2 s then returned to the voltage at which the spectra were scanned.

IV. METHYLPYRIDINES

Introduction

The 2-, 3-, and 4-methylpyridines were studied with SERS and compared to their normal solution Raman spectra, NSRS. The relative intensities and shifts of the observed transitions were investigated. The effect of varying the substituent as well as a detailed analysis of the effect of adsorption on different types of vibrations and their intensities was carried out. This analysis has interesting implications for the validity of some of the theories proposed to explain the effect. The results are also compared to those for 2-, 3- and 4-cyanopyridines [60].

Results

The bands of the NSRS and SERS spectra for the 2-, 3- and 4-methylpyridines are tabulated in Table 1 with their relative intensities in parentheses, as well as their assignments [59]. (See Figure 2 for the spectra.) The enhancement factor is on the order of 10^4-10^6. However, the transitions are not uniformly enhanced, but there is considerable variation from line to line. To simplify the discussion of relative intensity, we have chosen the symmetric ring breathing mode, 8, as having an intensity of 100 and compare all other band intensities to this one. (With the exception of the 812 cm^{-1} band in the NSRS of 4-methylpyridine which is slightly more intense than the 1011

Table 1. Observed frequencies and intensities of 2-,3- and 4-methylpyridine in normal and surface enhanced Raman spectra.

Design-nation*	4-Methylpyridine NSRS	4-Methylpyridine SERS	3-Methylpyridine NSRS	3-Methylpyridine SERS	2-Methylpyridine NSRS	2-Methylpyridine SERS
ν_1		3058 (9)		3060 (4)		[3061] (16)
ν_2		3042 (2)		[3037] (3)		[3061] (16)
ν_4	1617 (15)	1618 (93)	1606 (9)	1604 (15)	1605 (9)	1604 (60)
ν_5	1506 (6)	1503 (9)	1487 (2)	1487 (3)		1485 (20)
ν_6	1231 (13)	1233 (27)	1196 (10)	1197 (17)		1134 (4)
ν_7	[1074] (19)	[1068] (43)	[1051] (49)	[1052] (22)	[1058] (74)	[1061] (61)
ν_8	1011 (100)	1018 (100)	1038 (100)	1037 (100)	1014 (100)	1017 (100)
ν_9	[812] (106)	[813] (71)	824 (25)	820 (15)	808 (65)	809 (88)
ν_{10}	530 (23)	538 (56)	540 (23)	541 (6)	555 (37)	568 (7)
ν_{11}	3070 (27)		3071 (9)		3075 (20)	
ν_{12}	2998 (4)	2988 (1)		[3037] (3)		
ν_{13}	1569 (3)	1564 (4)	1587 (4)	1585 (9)	1578 (12)	1570 (16)
ν_{15}				1361 (2)		1378 (22)
ν_{16}		1284 (2)			1304 (8)	1299 (27)
ν_{17}		1101 (1)	1127 (3)	1126 (15)	1111 (7)	1110 (10)
ν_{19}	673 (19)	673 (14)	645 (6)	649 (12)	641 (12)	645 (25)
ν_{20}		972 (4)				985 (12)
ν_{21}		[872] (2)				
ν_{22}		390 (2)		406 (2)		399 (5)
ν_{23}		980 (4)				
ν_{24}	[812] (106)	[813] (71)	807 (5)	813 (4)		769 (5)
ν_{25}	725 (3)	722 (4)	712 (2)	707 (1)		725 (5)
ν_{26}	492 (4)	490 (9)			478 (4)	476 (1)

Design-nation*	4-Methylpyridine NSRS	4-Methylpyridine SERS	3-Methylpyridine NSRS	3-Methylpyridine SERS	2-Methylpyridine NSRS	2-Methylpyridine SERS
m_1	1222 (22)	1218 (91)	1235 (12)	1235 (8)	1246 (44)	1245 (76)
m_2	350 (4)	352 (2)	345 (3)	351 (1)	371 (4)	385 (5)
m_3	220 (10)	225 (29)	224 (12)	222 (7)	215 (34)	225 (27)
M_1	2935 (21)	2921 (26)	2936 (9)	2923 (5)	2938 (25)	2898 (9)
M_3	1387 (12)	1383 (45)	1390 (6)	1387 (5)	1388 (16)	1389 (9)
$M_4(b_1)$	1424 (2)	1439 (9)		1417 (2)		
$M_4(b_2)$					1435 (4)	
$M_6(b_1)$	[1074] (19)	[1068] (43)	[1151] (49)	[1052] (22)	[1058] (74)	[1061] (61)
$M_6(b_2)$		1165 (3)			1160 (7)	1160 (4)

*See ref. 7. ν_{1-19} are in-plane vibrations. ν_{20-26} are out-of-plane vibrations. m_1 is methyl stretch, m_2 is in-plane methyl deformation, m_3 is out-of-plane methyl deformation. M_1 is methyl CH symmetric stretch, M_2 is methyl asymmetric stretch, M_3 is symmetric HCH deformation, M_4 is HCH asymmetric deformation, $M_6(b_1)$ is in plane methyl wag and $M_6(b_2)$ is out-of-plane methyl wag.

[ ] frequency assigned more than once

( ) intensity relative to ν_8 which is assigned 100.

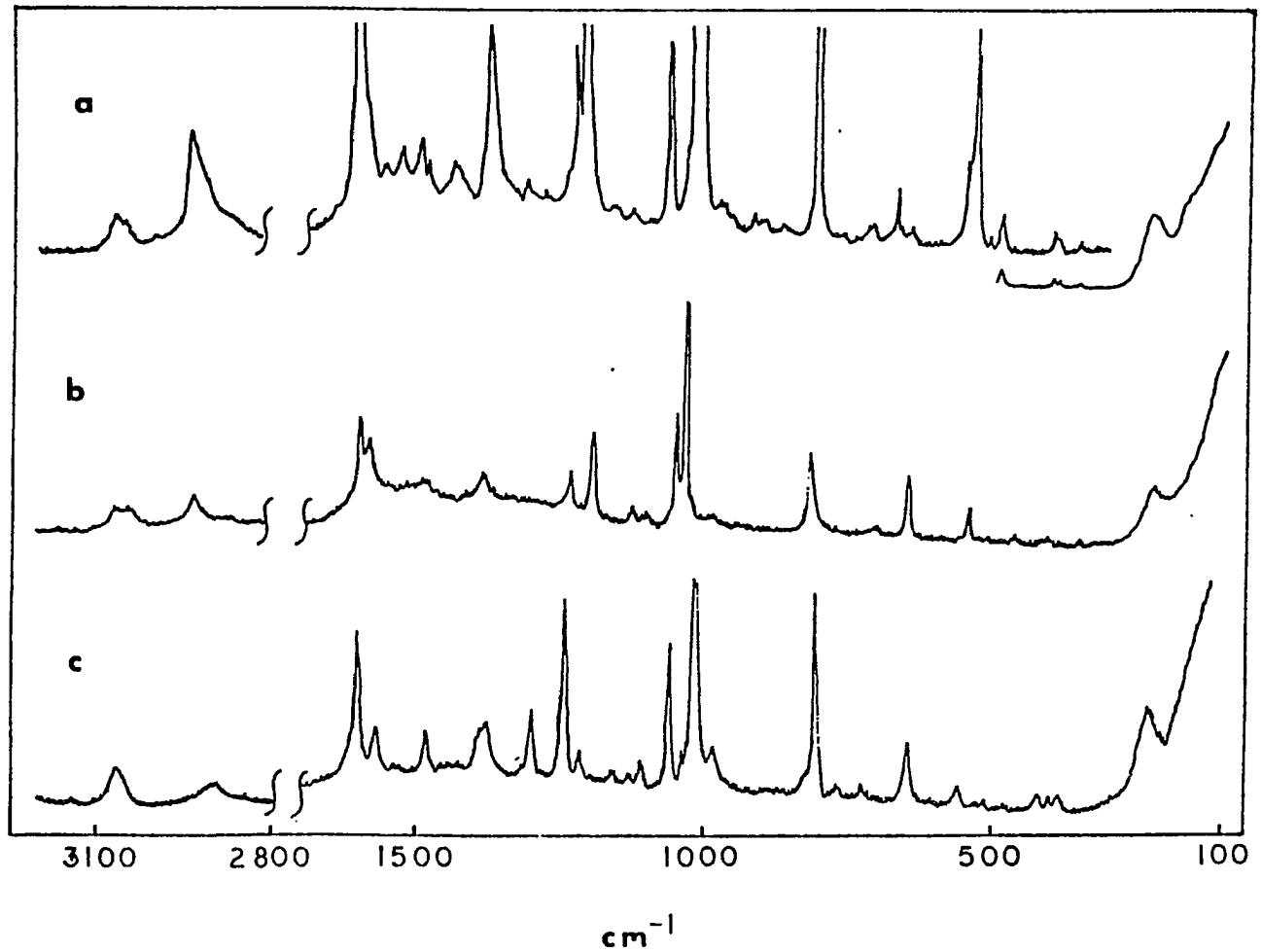

Figure 2. SER spectra of (a) 4-methylpyridine, (b) 3-methylpyridine, and (c) 2-methylpyridine.

cm^{-1} band, the ring breathing vibration is the most intense band in all the spectra.)

A second factor which must be considered in the band intensity comparison is that the NSRS are taken in dilute salt solutions to best reproduce the conditions of the SERS. Therefore several bands which normally appear in neat Raman spectra are not observed in the NSRS but do appear in the SERS.

Aside from changes in intensities some bands also shift and some broaden. The resolution is 2 cm^{-1} and most bands shift less than 5 cm^{-1}. Some of the bands that show larger shifts are M_4, asymmetric HCH deformation for 4-methylpyridine, M_1, methyl stretch for 2-, 3- and 4-methylpyridine, and 10, m_2, in-plane methyl deformation, and m_3, out-of-plane deformation for 2-methylpyridine. The M_1 band at 2938 cm^{-1} in the NSRS of 2-methylpyridine shifts to 2898 cm^{-1} and the SERS and broadens from 16 cm^{-1} (full width at half-height) to 44 cm^{-1}.

Discussion

The orientation of adsorbed pyridine with respect to the electrode surface has not been definitely determined. Most of the work to date has involved compounds containing nitrogen with an available unshared pair of electrons but the enhancement is observed with aliphatic as well as aromatic compounds [7]. This implies that bonding is not

necessarily through the π system. In a molecule such as methylpyridine, there is evidence that the molecule is adsorbed end-on involving the unshared pair of electrons on the nitrogen, in the σ system. If the methyl group is considered to have cylindrical symmetry, then 4-methylpyridine has C_{2v} symmetry. The 3- and 2-methylpyridines have C_s symmetry. For the discussion and assumption of end-on bonding to the electrode we define the z-axis as in the plane of the molecule and perpendicular to the electrode surface, the y-axis in the plane of the molecule and parallel to the electrode surface and the x-axis perpendicular to the plane of the molecule and parallel to the electrode.

For 2-methylpyridine, end-on bonding to the electrode through the nitrogen unshared pair of electrons may cause methyl-electrode interactions. The spacing of the silver atoms is sufficiently large that if the nitrogen forms a chemical bond with one silver atom, a methyl hydrogen could approach very close to its neighboring silver atom. Allen and Van Duyne, in their discussion of 2-cyanopyridine [60], tilt the molecule on the surface 9 degrees from perpendicular because, for that molecule, the bonding may be through both nitrogens. For 2-methylpyridine the molecule may adjust through tilting or by deformation of either the methyl CH bonds or the pyridine-methyl CC bond. If the nitrogen is no closer to a silver atom than the van der Waals radii, there is no need for distortion.

The M_1, methyl CH stretching vibration, for 2-methylpyridine shifts and broadens in the SERS compared to the NSRS. The NSRS band at 2938 cm^{-1} is 16 cm^{-1} full width at half-height and the SERS band at 2898 cm^{-1} is 44 cm^{-1} wide. The M_1 vibrations for the 3- and 4-methylpyridine do not show this large broadening. The 3-methylpyridine line at 2936 cm^{-1} in NSRS is 21 cm^{-1} wide and the line at 2923 cm^{-1} in the SERS is 20 cm^{-1} wide. The 4-methylpyridine NSRS 2935 cm^{-1} line is 20 cm^{-1} wide and the SERS 2921 cm^{-1} line is 35 cm^{-1} wide. However, this band is asymmetric, therefore it is probably due to two separate transitions. (The intensity of the 2- and 3-methylpyridines decreases in the SERS, but that of 4-methylpyridine remains relatively unchanged which also indicates it may be due to two separate transitions.) The broadening of the 2-methylpryidine line could be due to one of three factors: a) the lifetime could be shorter, but this is not likely because all the lines in the spectrum would be broadened, b) it could be split into two bands with exactly the same intensity, and c) the substituent could have an interaction with the electrode surface. This broadening would not be observed in the 3- and 4-methylpyridines because the methyl groups do not come near the electrode surface. The shifts of the M_1 band in 3- and 4-methylpyridine of -12 and -14 cm^{-1} respectively are significant, but the shift of -40 cm^{-1} for this band for 2-methylpyridine shows this vibration to be strongly affected by adsorption on the electrode. We see a similar trend with

the m_2 and m_3 vibrations, where the shifts in frequency are similar for 3- and 4-methylpyridine and are larger for 2-methylpyridine. The M_4, asymmetric HCH deformation, shows a large shift for 4-methylpyridine, but this vibration does not appear in the 2- and 3-methylpyridines for comparison. Band 10 shows a shift of 13 cm^{-1} for 2-methylpyridine. This vibration involves a ring deformation that may result in a stronger methyl-surface interaction than other modes. Whatever the interaction, whether deformation of methyl CH bonds or pyridine-methyl bonds, it is not sufficient to prevent observation of the SERS for 2,6-dimethylpyridine, the topic of the next chapter.

Allen and Van Duyne [60] have noted the enhancement of bands having a large component of the dipole moment in the z axis. With one exception, the vibrations of the 4-methylpyridine which have large components of vibrational motion along the z axis are enhanced in the SERS relative to the NSRS. The enhanced vibrations include 1, 3-6, 10 and 17. Those vibrations which have large components in the y axis are less enhanced. Other vibrations which have components in both the y and z directions show variable enhancement. For the 2-, 3- and 4-cyanopyridines Allen and Van Duyne [60] calculate the expected intensity ratio of the cyano stretch to the ring breathing mode using the relation

$$I_{CN}^{SERS}/I_{ring}^{SERS} = \cos^2\theta \; I_{CN}^{soln}/I_{ring}^{soln} \quad (1)$$

where θ is the angle between the CN bond axis and the z axis

perpendicular to the metal surface. We can use this equation to calculate the intensity of the M_1 band, the symmetric methyl CH stretch, for the SERS. Using 0, 60 and 120 degrees for θ for 4-, 3- and 2-methylpyridine respectively, the calculated results agree very well with the actual results as shown in Table 2. In the calculation for 2-methyl pyridine we ued 120 degrees, which is the angle when there is no distortion or tilting of the molecule. If the molecule is tilted 9 degrees as used for 2-cyanopyridine [60], then the value for $I^{soln}_{CH_3}/I^{soln}_{ring} \cos^2\theta$ is 0.032 and the argument still holds.

A second group of bands which are similarly enhanced, for 4-methylpyridines are those involving out-of-plane bend, 20-26, and m_3 except 24. The band at 812 cm^{-1} is simultaneously assigned for 24 and 9, and should be enhanced for both of these vibrations, but actually has lower intensity. This is the only exception. A similar enhancement of out-of-plane bending vibrations has been previously observed for pyrazine [36].

For 3- and 2-methylpyridine the symmetry of the molecule is reduced so that there are very few vibrations which can be said to have clearly a large z component. However, the out-of-plane vibrations are not affected by this reduction in symmetry. The 3-methylpyridine out-of-plane vibrations are less enhanced while most of the out-of-plane vibrations which do appear for 2-methylpyridine are

Table 2. Calculated and Experimental Raman intensities of the methyl CH stretching vibrations in SER spectra of methylpyridines.

Compound	θ(deg)	$\cos^2\theta$	$I^{soln}_{CH_3}/I^{soln}_{ring}$	$I^{SERS}_{CH_3}/I^{SERS}_{ring}$
4-Methylpyridine	0		0.21	0.26
3-Methlypyridine	60		0.0225	0.05
2-Methylpyridine	120		0.0625	0.09

enhanced. These include 20, 22, 24, and 25; 26 and m_3 are two exceptions, but m_3 may show less enhancement due to methyl-electrode surface interactions since it involves methyl out-of-plane deformation.

The reason for the selective enhancement of these out-of-plane vibrations for the 2- and 4-methylpyridines may be a larger polarizability in the x direction. These two methyl pyridines can delocalize more electrons into the system via hyperconjugation than the 3-methylpyridine. This would cause a large polarizability derivative in the x direction.

If the molecules are oriented perpendicular to the surface, the enhancement observed in vibrations which are entirely out-of-plane (x axis) are inconsistent with the image-dipole theory which has been suggested by several authors as an explanation of the observed enhancement [38,49]. According to these theories Raman scattering from an adsorbed molecule arises from both a dipole induced in the molecule and from the image dipole of that olecule within the metal surface. For dipole components parallel to the metal surface, the image dipoles oscillate out of phase and cancel, whereas dipoles oscillating perpendicular to the metal surface are in phase and contribute to the enhanced signal. As a consequence, only vibrational modes which have dipolar components perpendicular to the surface will show an enhancement and the magnitude of the enhancement will be

proportional to the projection of the dipole onto the z axis. We have shown both these conclusions to be correct for the in-plane modes of vibration of the methyl pyridines. Modes with large dipoles in-plane along the z axis are more enhanced than those with large y axis components (relative to 8) and the intensity of the vibration is proportional to $\cos^2\theta$ as is shown in Table 2. However, we also see enhancement in these modes of 2- and 4-methylpyridine which have dipole components entirely parallel to the surface. We have previously made this observation in pyrazine [36] where out-of-plane modes appear on the surface although they are forbidden (and not observed) in solution. In order to eliminate the inconsistency with the image dipole theory we could assume the molecules are tilted with respect to the z axis. In this situation the ratio of enhancement factors for out-of-plane vibrations to in-plane vibrations should be proportional to $\tan^2$, where is the angle of tilt of the molecular plane. We observe this ratio to be greater than 1 which would indicate a tilt angle of more than 45 degrees.

The classical Raman scattering theory of Efrima and Metiu [39] accounts for the giant enhancement by both an image dipole (self-polarization) effect and a resonance Raman effect. Calculations [39] given for the non-resonance case predict that the intensity of scattered light for a mode having a dominant perpendicular polarizability component will be an order of magnitude larger than for the parallel case. Our results show that t.. ffect of the

surface leads to a relative enhancement of many parallel modes with respect to perpendicular modes which again is inconsistent with this theory unless the molecules are tilted more than 45 degrees.

V. 2,6-LUITIDINE

Introduction

The exact nature of the molecule-electrode interaction is not yet well understood. This is partly because there is as yet insufficient data on the nature of the surface after pretreatment. It is known, for example, that roughening the surface enhances the spectral intensity, but the scale of the needed roughness is not known. Nor is it known why such roughening is necessary. It is likely that this question is related to the particular type of interaction between the adsorbed molecule and the surface. It is usually presumed that a pyridine-like molecule is attached to the surface through the interaction between the lone pair, non-bonding, electrons of the nitrogen atom and some orbitals in silver which are geometrically available for formation of at least a weak chemical bond. This model requires that the plane of the molecule be perpendicular to the surface [61]. Part of the evidence for this model comes from the appearance of a low-lying spectral line which has been attributed to the Ag-N stretching vibration [7,12,16,22-3,36,38,61-2].

We thus felt it worthwhile to examine the SERS of 2,6-lutidine (2,6-dimethylpyridine) to determine whether the placement of two rather bulky methyl groups adjacent to the N atom would effect the nature of the molecule-metal interaction. The spectrum would then be expected to differ from other SER spectra, perhaps exhibiting vastly reduced

intensities, shifted vibrational frequencies, especially of the methyl groups, or elimination of the Ag-N line. In fact, we see none of these effects. A spectrum is observed which is as intense as that of pyridine, the relative intensities and frequencies are shifted no more than those observed in other SER spectra, the Ag-N line appears, and the methyl stretches and bends are only slightly perturbed by the surface interaction. We also examine the geometrical consequences of these observations with respect to the nature of the surface-molecule interaction.

Results

The observed frequencies and intensities of the SERS and the NSRS (normal solution Raman spectrum) of 2,6-lutidine are given in Table 3. The spectral assignments are from Medhi and Mukherjee [63]. Most of the lines of the SERS are very similar to their NSRS counterparts; the largest shift observed is 15 cm^{-1} with the average shift around 6 cm^{-1}. The shifts are both to larger and smaller wavenumbers. Since the observed intensities are roughly the same as observed in this laboratory under the same conditions for the SERS of pyridine, the enhancemant factor for 2,6-lutidine is roughly the same, approximately 10^6, assuming the surface coverage to be the same.

Several of the methyl C-H vibrations are doubled in the SERS. (See Table 4.) That is, two bands appear where only one or no bands appear in the NSRS. For example, M_3, the

Table 3. Observed frequencies of 2,6lutidine in normal and surface enhanced Raman spectra.

Mode number [22]	NSRS[a]	SERS[a]
16b	206	210h
18b		220m
10a	300	312w
		408vw
16a	430	432vw
6b	541	542w
6a	566	566w
		647w
4	723	728s
16b		752w
		815bm
		976bm
1	1008	1010m
	1037	1036vs
M_6	1050	1052m
18a	1099	1103w
15		1143w
	1162	1170w
M_6		1196m
7b		1213w
3		1234m
13	1271	1272s
M_3	1382	1372m
	1409	1398m
19b		1416w
M_4	1442	1445vw
M_4		1455vw
8b	1584	1584m
8a	1603	1601s
		2825vw
	2863	2877v
		2890vw
M_1	2932	2922w
20a,b		3043w
2	3074	3062w

NSRS solution concentrations were 2M 2,6-lutidine and 0.1 M KCl
SERS concentrations were 0.05M 2,6-lutidine and 0.1 M KCl.
h=shoulder, b=broad, vs = very strong, s = strong, m = medium,
w = weak, vw = very weak
M_1 = CH_3 symmetric stretch, M_3 = CH_3 symmetric deformation,
M_4 = CH_3 asymmetric deformation, M_6 = CH_3 rock.

Table 4. Doubling of Methyl Vibrations.

Band[22]	NNRS cm^{-1}	Liquid IR cm^{-1}	NSRS cm^{-1}	SERS cm^{-1}
M_6	1044	1029		1052
	1190	1193		1196
M_3	1374	1375	1382	1372
				1398
M_4	1445		1442	1445
		1455		1458

methyl symmetric deformation, has only one assignment in the neat normal Raman spectrum (NNRS) or IR spectrum, but on the surface this band splits and appears at 1372 and 1398 cm^{-1}. This doubling is not voltage dependent; the bands appear at 1372 and 1398 cm^{-1} for potentials between -0.6 to -0.9 V. However they do not appear at voltages more positive than -0.6 V. M_4, the methyl assymetric deformation, has two bands assigned, one each in the Raman and IR spectra at 1445 and 1455 cm^{-1} respectively. Both of these bands appear in the SERS, at 1445 and 1458 cm^{-1}. M_6, the methyl rock, has two assignments in the NNRS, at 1044 and 1190 cm^{-1}, neither of which appears in the NSRS, but they both appear in the SERS at 1052 and 1196 cm^{-1}.

In the 200 cm^{-1} region of the NNRS there are two lines assigned to molecular vibrations [63]. These are 16b at 200 cm^{-1} and 18b (methyl sensitive) at 218 cm^{-1}. In the NSRS these are observed at 208 and 218 cm^{-1} and in the SERS these are observed and almost resolvable at 210 and 220 cm^{-1}. However, in the SERS these bands are on top of a broad feature, probably centered around 215 cm^{-1}. The relative integrated intensity of the 215 cm^{-1} feature to the 725 cm^{-1} band in the NSRS is 1.2 while in the SERS this ratio is about 2.5, indicating the probability of another vibrational band in this region. We assign this broad feature to Ag-N vibration based on numerous other works [7,12,16,22-3,36,38,61-2].

There is also an appearance of a strong, sharp band in the SERS at 1035 cm^{-1}. Of the two possible assignments from comparison to the neat Raman spectrum, neither seems quite appropriate. One possible assignment is 1374-342 cm^{-1} = 1032 cm^{-1}, a difference band. (In the SERS this would be 1372-312 = 1060 cm^{-1}.) But the 1035 cm^{-1} band is stronger than the 1372 and 312 cm^{-1} bands. It could be the 1044 cm^{-1}, M_6, in-plane methyl rock. However, it has a very different voltage dependence than the other bands, and is quite sharp, 5 cm^{-1} full width at half-height, compared to a width of about 10 cm^{-1} for most other bands. It seems to have similar behavior to the 1025 cm^{-1} band which appears in the pyridine SERS at -0.6 V [6,64] and disappears at more negative potentials. Takenaka [65] assigns this to the totally symmetric ring breathing band of pyridine bonded directly to the electrode as opposed to the 1008 cm^{-1} band due to the totally symmetric ring breathing mode of pyridine hydrogen bonded to water adsorbed on the electrode surface. However, the 1035 cm^{-1} band is probably not due to a vibration of the 2,6-lutidine on the electrode surface because it is narrower than the 1008 cm^{-1} band in the NSRS, and the bands in the SERS are usually broadened.

There are two strong bands in the 3,5-lutidine SERS at 1037 and 752 cm^{-1}; the 1037 cm^{-1} band is the strongest in the spectrum and the 752 cm^{-1} band next strongest. It is possible that the 1035 cm^{-1} and 752 cm^{-1} bands in 2,6-lutidine are due to a small im_urity of 3,5-lutidine, in

spite of our efforts to remove the impurity by frsactional distillation.

Discussion

The most notable result of the SERS of 2,6-lutidine is that enhancement is found at all. If the molecule is adsorbed on the electrode in an end-on fashion through the unshared pairs of electrons on the N, then the two methyl groups offer significant steric hindrance. If the bonding is through Ag-N, then the Ag-N distance would be expected to be longer or the methyls distorted to accommodate their bulk. One possibility for alleviating this steric hindrance could be surface roughness on an atomic scale. We first examine the methyl vibrations for evidence of geometrical distortion, then we discuss the Ag-N bond, and finally the implication of these results for the nature of the Ag surface.

Several of the methyl vibrations were observed to be doubled slightly. (See Table 4.) This implies that either each methyl group could be in a slightly different environment, or that the methyl vibrations could couple when adsorbed on the surface. However, there are four intervening bonds between the C-H's of the methyls, a rather long distance for coupling [66]. Of particular note is that the separation of the 1372 and 1398 cm^{-1} bands is voltage independent. Apparently whatever the cause for doubling, changes caused by varying the voltage, such as orientation

or surface-molecule distance, do not affect the doubling. The conclusion which can be drawn from the small shifts in the methyl vibrations, as well as the small doubling, is that the methyl vibrations are simply not strongly affected by adsorption on the electrode.

Some models for 2,6-lutidine adsorption on the electrode are illustrated in Figure 3. Theoretically, there are many possible orientations but whatever the orientation, we must allow for, at most, only small distortion of the methyl groups. In previous work derived from solution thermodynamic properties with pyridine adsorbed on Hg [67,68], it has been concluded that the moldcule lies end-on with the nitrogen away from the electrode or flat on the surface. However, these models do not necessarily imply that pyridine, or pyridine-type molecules orient themselves the same way on silver. The appearance of a line of 230 cm^{-1} which has been attributed to the Ag-N stretch is evidence that the molecule is oriented with its plane perpendicular to the surface and the N adjacent to the surface.

There is some dispute in the literature as to whether the band around 230 cm^{-1} is due to Ag-N vibration. Some of the evidence that this band is due to a pyridine vibration, whether pyridine-metal, pyridine-water, or pyridine-chloride, is that it appears only when pyridine is added to the cell and shows similar intensity dependence on

pretreatment as the 1008 cm^{-1} band which is due to pyridine symmetric ring breathing [69]. The 230 cm^{-1} line shows the predicted voltage dependence for an Ag-N bond; as the voltage is made more negative the 230 cm^{-1} line shifts to lower frequency [22]. However, Dornhaus and Chang [69] have observed peaks at 86 cm^{-1}, 161 cm^{-1} and a shoulder at 110 cm^{-1} but no peak near 244 cm^{-1} for Ag-pyridine-NO_3 crystals. Note that this cannot be taken to mean that the peak around 230 cm^{-1} is not the Ag-N stretch, since, in the complex, the Ag has a full positive charge and there sould be little reason to expect the same vibrational frequency as a neutral Ag-N interaction. Other evidence for bonding through the N rather than the system of pyridine is that a system is neither necessary nor sufficient for observing SERS; SERS including a line around 230 cm^{-1} are observed for piperidine, [70] not benzene. The SERS of the 2-,3- and 4-methylpyridines also point towards Ag-N bonding. The methyl vibrations shift more for the 2-methylpyridine than for the 3- and 4-methylpyridines indicating steric hindrance for the 2-methylpyridine. The out-of-plane vibrations are enhanced for the 2- and 4-methylpyridines but not the 3-methylpyridine. This is attributed to hyperconjugation resulting from the the N being electropositive due to the delocalization of the unshared pair of electrons to Ag [61]. The experiments of Tsang and Kirtley on 4-aldehydepyridine adsorbed between Ag and aluminum oxides with the N bonded to Ag also point towards Ag-N bonding [71].

The question whether the band around 230 cm^{-1} is due to Ag-N is complicated by the fact that 2,6-lutidine has two assigned molecular vibratons in this region, namely 16b and 18b. We observe a single broad peak with two features in this region centered at 215 cm^{-1}. It is considerably broader than the other SERS lines which indicates it is most likely composed of several lines. In shape, width and intensity it is very similar to previously observed Ag-N surface lines in which the molecules had no interfering lines in this region [22,36]. Its integrated intensity is greater than what would be expected if it were composed of only the two assigned vibrations 16b and 18b. It is also too wide (40 cm^{-1}) to be only two normal vibrations. We have shown that the Ag-N line is usually more than 30 cm^{-1} in width and inhomogenously broadened [22] as well as somewhat skew. These features are also apparent in the line observed in 2,6-lutidine, and we take this as evidence that despite the interference of other spectral lines in this region, the nature of the observed line is sufficiently similar in characteristics to other Ag-N lines that we may, with some confidence, conclude it is present here as well.

If there is a silver-nitrogen bond, no matter how weak, then the molecule must certainly orient itself in some end-on fashion where the nitrogen can bond to the electrode. A chemical bond requires reasonable orbital overlap between the orbital containing the unshared pair of electrons on N and the Ag orbitals. Unfortunately, too little is known

about orbitals of the silver surface.

We have set up a geometrical model to explore the consequences of the above observations for the nature of the molecule-surface interaction. It is not yet known whether this interaction should be described by physisorption, in which case we should expect van der Waals radii to be important, or chemisorption, in which case we should use covalent bond lengths to describe the Ag-N interaction. Considering 215 cm^{-1} as a lower limit to the bond dissociation energy (no overtones have been observed) we might expect the situation to be somewhat in between. However, no vibrational fundamental would be observed for a pure van der Waals interaction. We may thus conclude that the sum of the van der Waals radii (0.15 nm for nitrogen and 0.1525 nm for silver) gives an upper limit to the Ag-N distance of 0.3 nm. (See Table 5 for pertinent radii and Figure 3.) In the limit of covalent bonding we should expect the Ag-N distance to be similar to other metal-nitrogen bonds, most of which are close to 0.19 nm [72]. At this distance, the bonding Ag atom is too close to the methyls and the Ag would strongly distort the methyl groups resulting in vastly different vibrational frequencies. If we raise the molecule farther from the surface so that the N-bonded Ag and methyl-C distance is the sum of their van der Waals radii, 0.35 nm, then the Ag-N distance is 0.25 nm. At this distance, however, the geometry is such that the methyl groups would still strongly interact with Ag atoms

Table 5. van der Waals radii and bond lengths.

van der Waals radii (Å)		Bond lengths (Å)
H	1.2	N-C 1.37
Me	2.0	C-Me 1.5
N	1.5	
Ag	1.528	

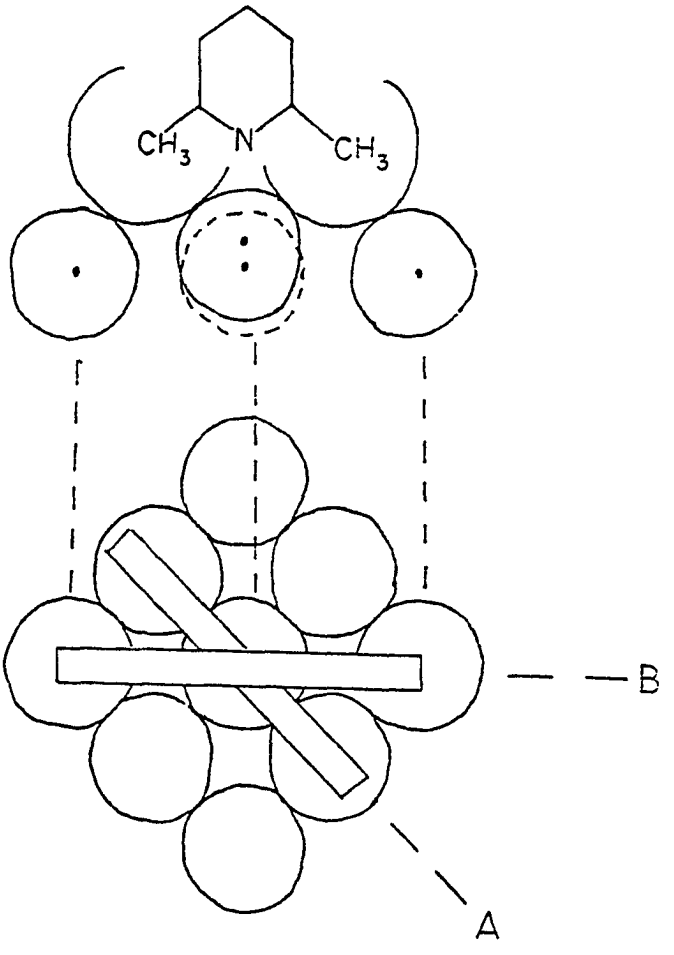

Figure 3. Model of 2,6-lutidine adsorbed on a silver surface. The lower figure is a top view looking down on the surface assuming a (100) plane is exposed. The rectangles are two possible orientations of the molecular plane. Orientation A is with the methyls over Ag atoms which are nearest neighbors to the (central) N-bonded Ag atom. Orientation B is with the methyls over Ag atoms on the diagonal. The upper figure is a side view of the molecule in orientation B, with the molecule now shown such that the Me-Ag distance is the sum of the van der Waals radii (see text). The N-bonded central Ag atom is shown in two possible positions. The first (dotted) is in the surface plane, and the second (solid) slightly raised (by 0.075 nm) to form a weakly covalent bond with the nitrogen.

neighboring the N-bonded atom. This picture assumes that all the surface Ag atoms lie in a common plane and that their separation is the same as the closest distance in the bulk metal (.2889 nm). Considerably less hindrance would be encountered by the methyls if the molecular plane is oriented across the diagonal of a square of silver atoms as might be expected to be exposed if the surface were along a (100) or a (110) plane. With this assumption we take the distance between Ag atoms in the molecular plane to be 0.41 nm ($= \sqrt{2} \times 0.889$ nm). This configuration places the C's of the methyl groups at a distance of 0.24 nm from the diagonal Ag, considerably less than the sum of their van der Waals radii (0.35 nm). This requires either severe distortion of the methyl groups, or a greater molecule-surface plane distance. The former is ruled out because we would expect to observe much larger shifts and splittings in the methyl vibrations than are in fact observed. However, if the molecule were as far away as the van der Waals radii, we would not see an Ag-N vibration in the spectrum. One way to explain these apparently contradictory observations is to assume that the surface is roughened on an atomic scale such that, at the surface enhanced sites, a bonding Ag atom lies somewhat above the plane of the nearest diagonal silver atoms. Assuming that the methyl and diagonal silver atoms are at least separated by the sum of their van der Waals radii, we find that we may raise the Ag atom by at most 0.075 nm above the surface before its own van der Waals

radius touches that of the methyls. At this point it is 0.25 nm from the N atom, still somewhat closer than the van der Waals distance, thus allowing considerable electron overlap. We thus take 0.25 nm as a lower limit to the Ag-N distance for the surface configuration in which the molecule is situated over the diagonal of a square. Still another possibility is that for part of the polycrystalline surface the (111) face is exposed. Then the 2,6-lutidine may be oriented across a still longer diagonal. In this configuration adjacent silver atoms are separated by 0.500 nm (= $\sqrt{3}$ x 0.2889 nm). Using similar geometric considerations we find in this case that a Ag atom need not be raised above the surface (no surface roughening is required) before its own van der Waals radius contacts that of the methyls. Under these circumstances the lower limit of the Ag-N distance is still 0.25 nm. These models of the surface-molecule interactions are consistent with all the observed spectral data.

Conclusion

To summarize, in order to observe a Ag-N stretch, the Ag-N distance must be less than the sum of the van der Waals radii. However, with a planar (100) or (110) surface, a covalent bond would require considerable distortion of the methyl groups resulting in larger spectral shifts than are observed. We thus must invoke surface roughness on an atomic scale, so that only sites where a silver atom is

raised above the surface plane result in an enhancement. The resulting Ag-N bond is weakly covalent with a length at least 0.25 nm. If the molecule is adsorbed on a (111) face, no surface roughness need be invoked. These models for suface roughness are in agreement with the conclusions of Furtak, Trott and Lee [73] and Billmann, Kovacs and Otto [74] that roughness on an atomic scale is important The latter authors invoke the idea of atomic scale roughness due to adatoms as sites for molecular adsorption. Such a model is consistant with the geometric arguments we have advanced to explain the 2,6-lutidine SER spectrum. Pettinger et al. [17] found no roughness required for observing SERS on a single crystal Ag (111) surface, but they found no roughness only on a scale greater than 10.0 nm. This does not exclude roughness on an atomic scale. The single crystal they used had a (111) surface, the face for which our model does not require roughness. Moskovits [12] proposes that the enhancement comes from adsorbate covered metal bumps, an almost undetectable micro structure, by which he is able to explain the excitation functions.

REDUCTION OF 4-ACETYLPYRIDINE

Introduction

Although one of the interesting aspects of SERS is the theoretical explanation of the mechanism, useful applications are the ultimate goals. Since SERS allows detection of vibrational spectrum of monolayers of adsorbed species on electrodes, looking for intermediate species or products of an electrochemical reaction may be possible and could lead to in situ identification of such species. Although the SER effect has been recently shown for Hg surfaces [75] it has not yet been shown for Hg electrodes. Thus there are some limitations on what type of reactions can be looked at since the potential at which hydrogen ion is reduced is less negative on Ag, about -1.3 V, than on Hg. Also many more electrochemical reactions have been investigated on Hg dropping electrodes because surface contamination can be reduced to a minumum, which is a problem on Ag electrodes. The reduction of 4-acetylpyridine was chosen to investigate using SERS because the reduction takes place at -1.14 V and forms mainly two products, 4-(1-hydroxyethyl)-pyridine (HEP) II, or 2,3-bis-(4-pyridyl)-2,3-butanediol (BPB) III, a pinacol. See Figures 4 and 5. The organometallic product picured in Figure 4 can also be produced at certain electrodes and can lead to the hydrocarbon I [76].

The first step in the reduction of ketones is the

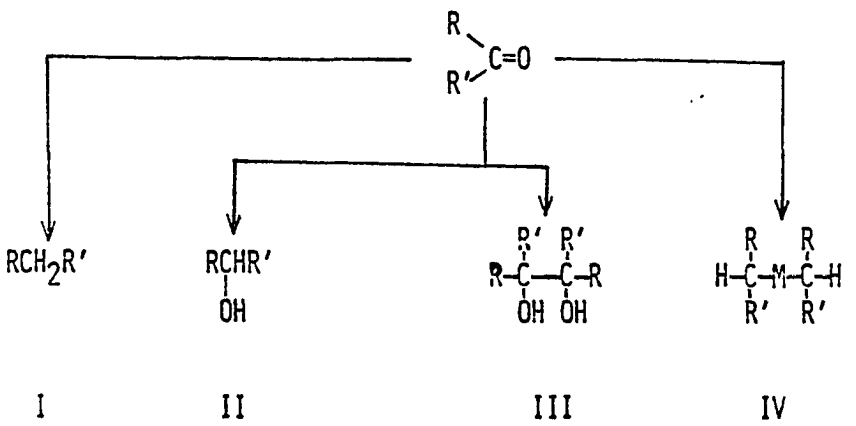

Figure 4. Possible reduction products for ketones: I. hydrocarbon, II. alcohol, III. Pinacol from bimolecular reductions, and IV. organometallic compound from reaction with the ketone and cathode.

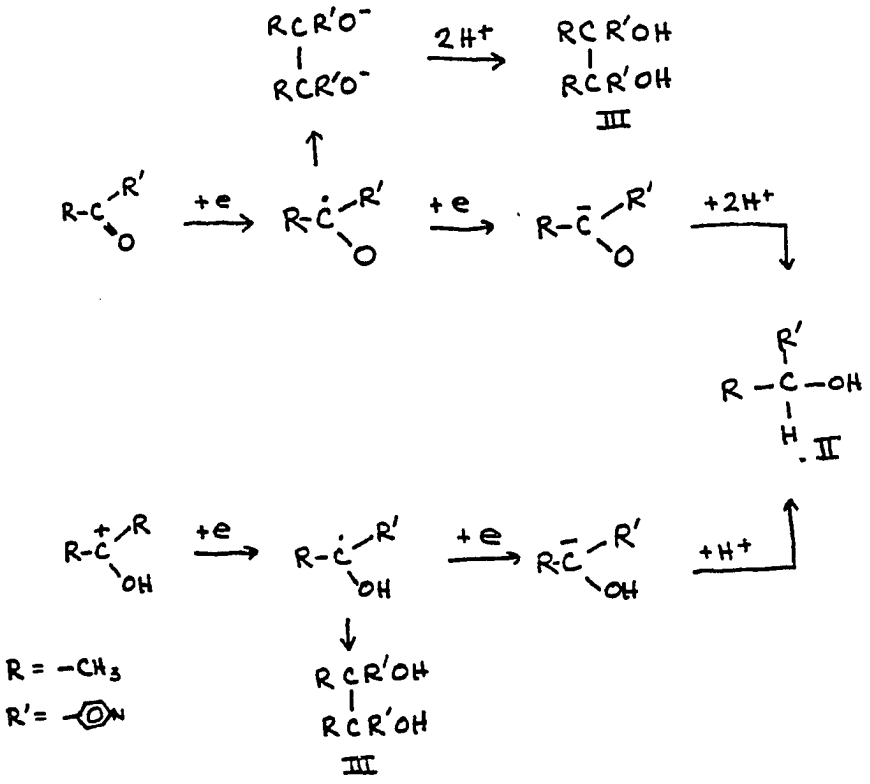

Figure 5. Possible reduction paths for ketones in basic (top) and acidic (bottom) media.

formation of the free radical $R_2\dot{C}OH$. In acid solution the radical formation is preceeded by protonization. In ketones protonization is slow and is responsible for the kinetic limitation of the first wave. Once the radical is formed, it can dimerize or pick up a second electron followed by protonization to form the secondary alcohol. (See Figure 5.) For an asymmetric ketone the alcohol can be optically active; the pinacol can exist as meso or racemic structures and can also undergo rearrangement to the pinacalone. Three factors affect the product obtained, the cathode material, current density, and pH of solution. To obtain high yields of alcohols a current density of 0.06-0.10 A/cm^2 is recommended, as well as moderately acid or alkaline solutions. Zinc gives high yields of alkanes. For the hydrodimerization of aromatic ketones water-alchol solutions of HCl, AcOK or KOH are recommended. Allen and Cahen report the quantitative yield of the dimer from 4-acetylpyridine on a mercury electrode [77].

It was thought [76] that the reduction of ketones on electrodes went through a chemisorbed complex involving the C+ of the carbonyl. However Brewster [78] makes some very interesting points concerning whether the chemisorption takes place at the O or C. See Figure 6. Species V and VI are sterically strained. Species VII and VIII are less strained and are additionally stabilized through the resonance with the aromatic pyridine ring. Dimerization can easily take place from species VII forming the pinacol.

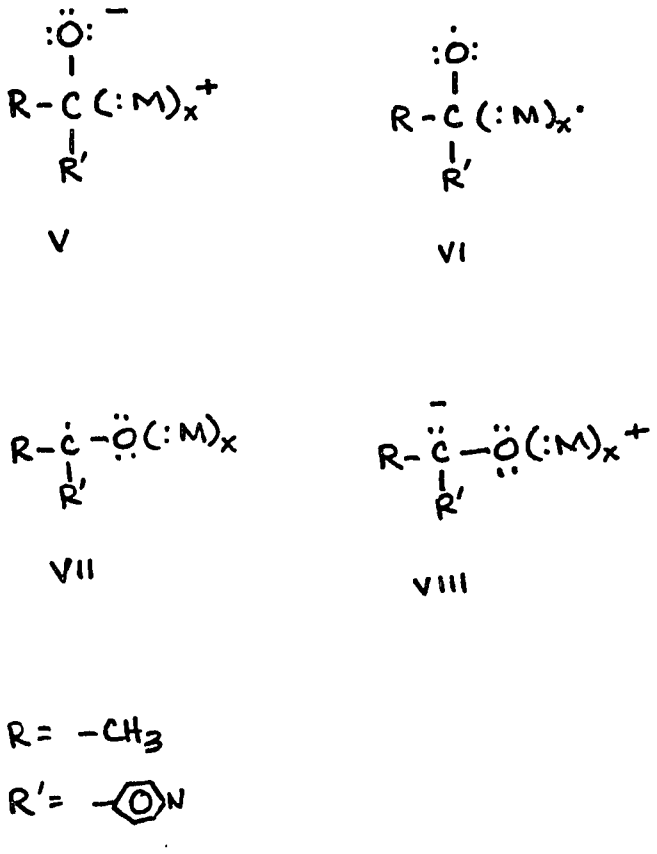

V VI VII VIII

Figure 6. Possible chemisorption intermediates in the reduction of ketones.

Species VIII can form the pinacol from reaction with dissolved ketone. To get the pinacol product from species V and VI, a more complicated mechanism is required. Species V would surely give the alcohol under acidic conditions. It was hoped that the technique of SERS would be able to show what surface complex does exist and to see which products are formed on the electrode. Combined with cyclic voltammetry it was hoped that the nature of the intermediate structures could also be determined.

Experimental

The BPB was synthesized and purified by the method of Bencze and Allen [79]. The HEP was synthesized as suggested by Taylor [80]. A mixture of 6 g 4-acetylpyridine and 0.95 g $NaBH_4$ in 50 ml water was stirred for 1/2 hour at room temperature. NaCl was added to aid in the extraction. A total of 75 ml choloroform was used for three extractions which were combined and dried over $MgSO_4$. The filtered solution was evaporated. The solid residue was distilled under vacuum and yielded 4.22 g which melted at 60-60.5° C. The 70% yield was more than sufficient for our requirements and experimental conditions were not optimized for better yield. NMR results were in good agreement with Freifelder [81].

Results and Discussion

The cyclic voltammogram (Figure 7) and the pulse

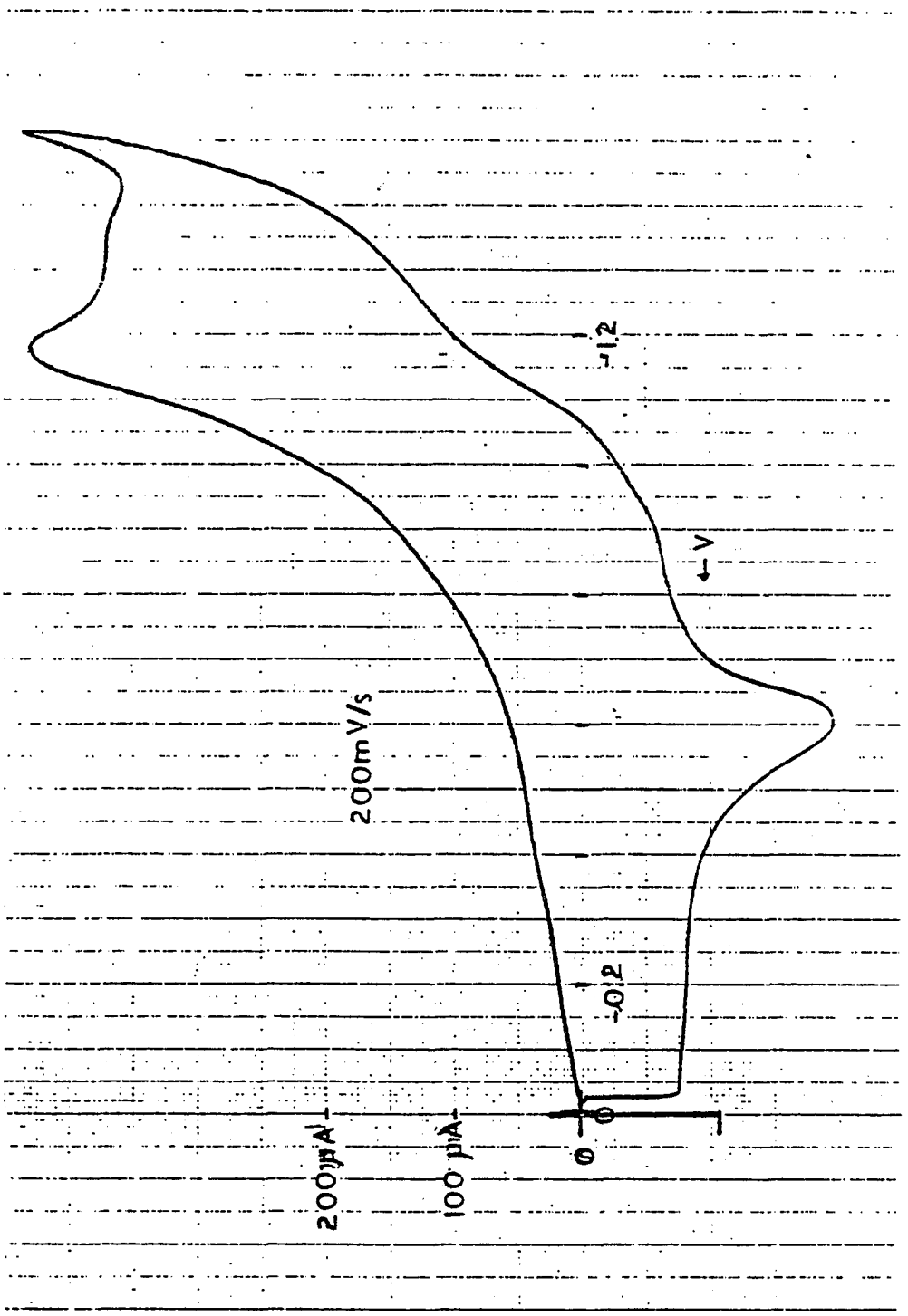

Figure 7. Cyclicvoltammogram of 4-acetylpyridine 0.05 M in 0.1 M KCl.

polarogram were taken of 4-acetylpyridine. These show that the reduction takes place in a single, irreversible wave at about -1.14 V. This comes near the potential for water reduction on the Ag electrode, but is clearly distinguishable.

The spectra of 4-acetylpyridine were taken at 0, -0.2, -0.3, -0.4, -0.6, -1.14, and -1.2 V on the Ag electrode and a normal Raman spectrum was taken of 2 M 4-acetylpyridine in 0.1 M KCl solution. The spectrum at the most negative potentials, -1.14 and -1.2 V, show many fewer lines. It was hoped that the spectra at the reduction potential would show intermediates or products of the reduction, but the spectra at -0.6 V of the starting material, 4-acetylpyridine, and the possible products, BPB HEP, and 4-ethylpyridine are not very different. It was also hoped to see the disappearance of the strong C=O stretch and the appearance of the alcohol vibrations. However, as in 4-pyridylaldehyde [82], there appears to be formation of hydrate which is preferentially adsorbed or is formed due to adsorption [83]. The C=O at 1693 cm^{-1} is a very strong band in the NSRS and is at 1695 cm^{-1} but very weak in the SER spectra. As weak as it may be, the 1695 cm^{-1} band is persistent until the potential of reduction is reached, at which point it disappears. After holding the potential at -1.14 V and returning to -0.6 V, the 1695 cm^{-1} band does return.

Synthesis of the product for analysis was attempted

through controlled potential electrolysis, however, the electrode appears to be coated with the product and the current quickly slows down so that a very small percentage of material is reduced. Since the dimer product, HEP, is very insoluble in water, whereas the alcohol is very soluble, this is indication that HEP is being produced.

The spectra of 4-acetylpyridine in H_2O and D_2O at -1.14 V are very similar. (See Figure 8.) The H_2O spectrum shows 1309, 902 and 788 cm^{-1} bands which do not appear in the D_2O spectrum and a 1056 cm^{-1} which is at 1050 cm^{-1} in D_2O. This band is the C-OH stretch. The D_2O spectrum shows bands at 766, 604, 305 and 351 cm^{-1} which do not appear in the H_2O spectrum. However, these bands are weak. The obvious differences in these spectra should be the OH and OD stretches and bends, and indeed, broad bands are seen in the H_2O spectrum around 3500 cm^{-1} and in D_2O around 2500 cm^{-1} However these spectra are not as intense as those obtained at -0.6 V for example, where these bands do not appear, so these broad bands due to OH and OD are probably due to the solution and not the adsorbed alcohol.

One of the more remarkable features in the spectra of 4-acetylpyridine at potentials below the reduction potential is the large variation with potential in intensity of the various vibrations. (See Figure 9.) These variations do not seem to follow any particular pattern as to type of vibration or symmetry. Not all vibrations are well

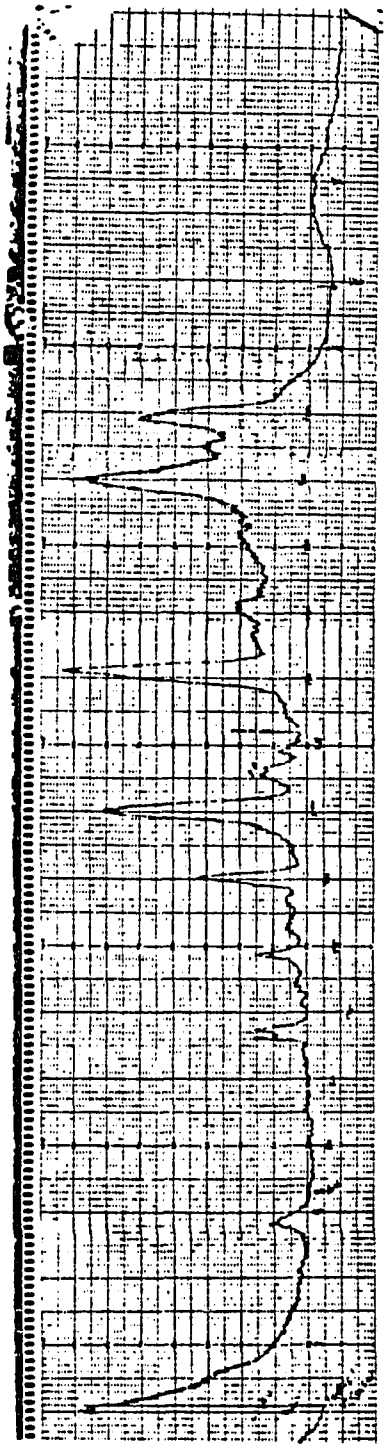

a. 4-acetylpyridine in H_2O at -1.14 V.

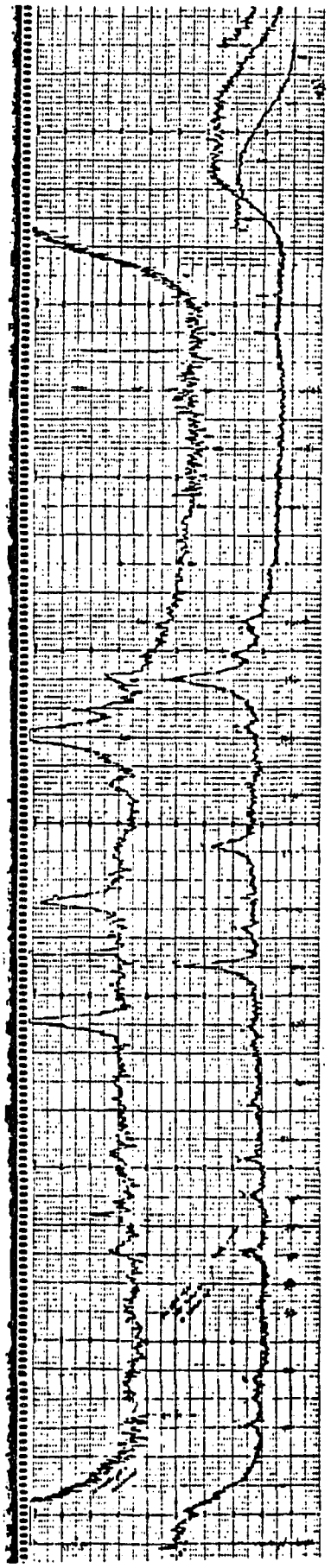

b. 4-acetylpyridine in D_2O at -1.14 V.

Figure 8. Comparison of spectra in D_2O and H_2O.

assigned, especially the lower cm^{-1} vibrations have no indisputable normal counterparts. In fact, no assignments for 4-acetylpyridine could be found and the best that could be done was to correlate spectra with acetophenone [84] and then correlate vibrations [85]. The bands (in cm^{-1}) which become relatively more intense with increasing potential are 297, 388 (possibly 6a, a_1, ring deformation), 662, 676, 904 (possibly CH out-of plane bend, 17b, b_1), 1202 (9a, a_1, CH in-plane deformation), 1308 (3, b_2, CH in-plane deformation), 1348 (14, b_2, ring stretch,) 1437 (methyl asymmetric deformation), and 1558 (8b, b_2, ring stretch). Those bands whic.. remain more or less relatively as intense are 1213 (OH deformation), 1272 (13, a_1, CH stretch), 1492 (19a, a_1, ring stretch). The shifts of the intensities of these bands at potentials below the reduction potential may be significant of a change in binding sites. The 4-acetylpyridine has the several possible bonding configurations mentioned, not only V-VIII but also through the pyridine N. From calculations [86] based on experimental re_ults, the frequency of the low-lying vibrations can be correlated to molecular weight and the atom bonded to the electrode, O, C or N. It would be interesting to see if the low-lying vibration did also shift with potential in order to ascertain if the bonding atom does indeed change. However, experimental evidence shows there is very little difference beetween O and C bonding on this low-lying band.

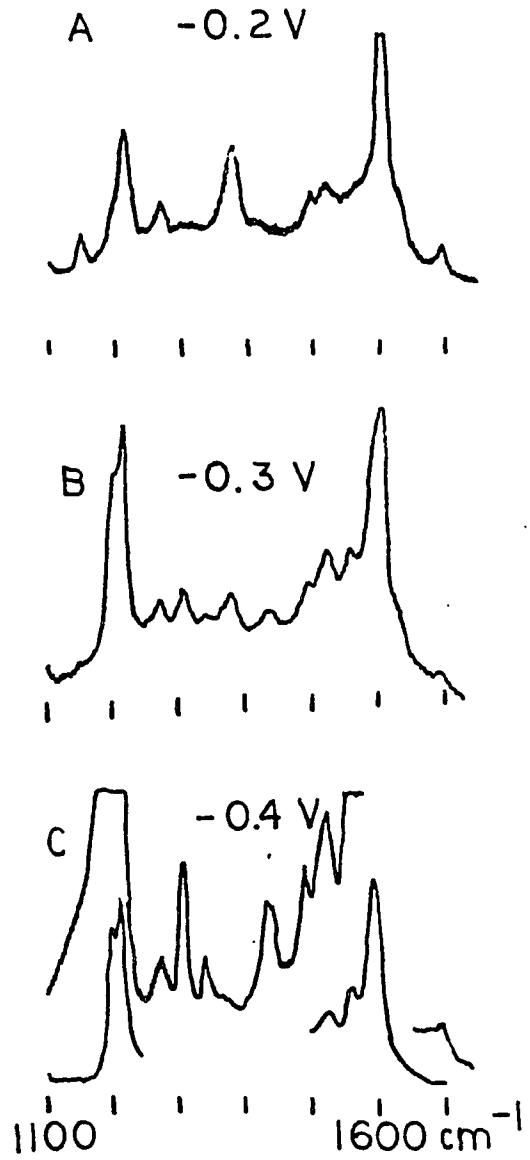

Figure 9. 4-acetylpyridine at various potentials. A) 1 x 10^4 c/s, B) 3 x 10^4 c/s and C) 3 x 10^4 and 1 x 10^5 c/s.

Figure 10 shows the spectra of 4-acetylpyridine, HEP, BPB and 4-ethylpyridine at -1.14 V. This figure clearly demonstrates the problem encountered with looking for intermediates and products of this reaction. The first spectrum could easily be the sum of starting material, intermediates and products but none of the bands are particularly distinguishable for indisputable identification. The DPB shows very little perhaps because of its low solubility. This could also be due to a difference in stereochemical conformation depending on whether the compound is produced electrochemically or photochemically. The meso conformation with intramolecular H-bonding has both pyridines syn while the racemate has them anti. Thus the low intensity may be due to the possibility that in the racemate only one of the pyridine rings can bond to the electrode. The 4-ethylpyridine also shows very little at this potential.

Conclusion

In spite of all the difficulties with using SERS to study the electrochemical reduction of 4-acetylpyridine, there is still much promise for this application of SERS. The shifts in intensity of the vibrations at different potentials may have important implications on bonding as well as what vibrations are relatively enhanced and why. The low intensity of photochemically synthesized DPB may have important implications on the relationship of molecular

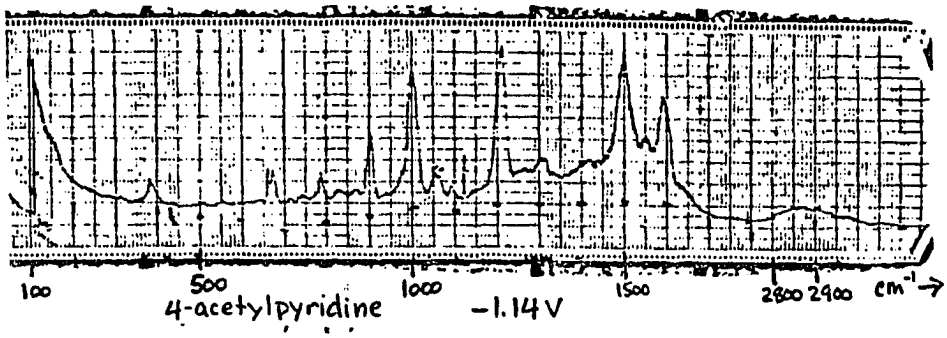

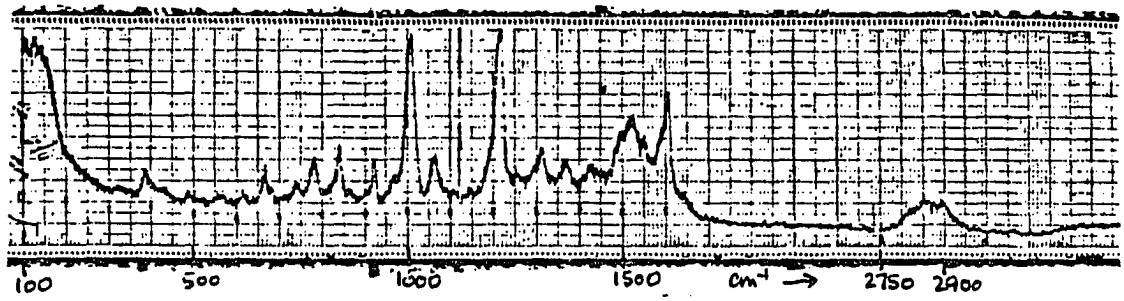

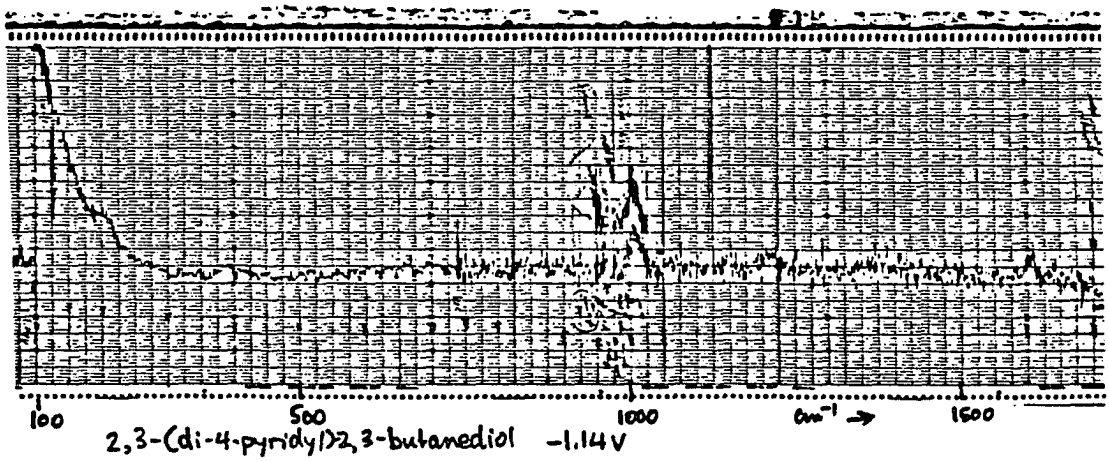

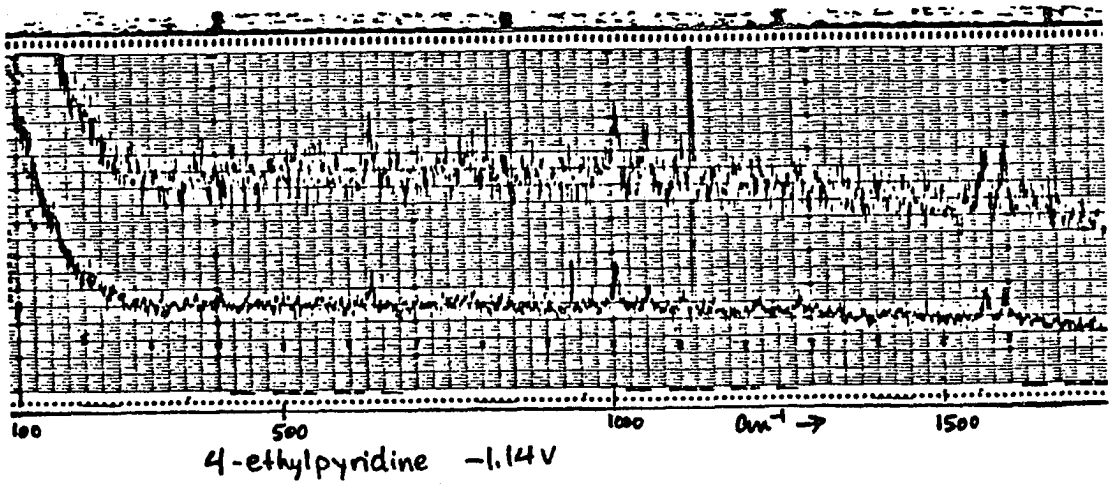

Figure 10.

structure and bonding on SERS. Whether both pyridines of bipyridial-type molecules need be bound to the electrode to see enhancement would have important implications on the theory. Finally, the changes in the 4-acetylpyridine spectrum at -1.14 V compared to lower potentials and the lack of positive correlation to one of the possible products may mean that we are indeed looking at steady state intermediates.

CONCLUSION

This work has several important implications for the nature and applicat_ s of SERS. The picoline analysis was the first to have complete vibrational assignments. This work shows that it is not only the vibrations with large components perpendicular to the electrode that are enhanced but also components parallel to the electrode. This is experimental evidence against a strict dipole image theory for enhancement. The fact that the out-of-plane vibrations for 2- and 4-methylpyridines are enhanced but those for 3-methylpyridine are not is further evidence that the bonding is through the N.

The 2,6-lutidine work shows experimentally that adatoms are an important roughness scale to be considered. This seems to be very important for the theoretical explanations and fits quite well with Otto's theory on adatoms.

The 4-acetylpyridine has many implications for SERS in terms of bonding and applications of SERS to stydying electrochemical reactions. This work also shows that water does not seem to show the SER effect.

This work is important in that it is experimental work that either confirms or disproves theories. It also shows that SERS is interesting for its useful applications and not just its theorey. This work also suggests many more experiments that need to be done before SERS is completely

understood and it becomes a routine labortory technique for studying the interaction between molecules and surfaces.

REFERENCES

[1] Albrecht, M. G.; and Creighton, J. A., J. Amer. Chem. Soc., 1977, 99, 5215.

[2] Van Duyne, R.P.; Jeanmaire, D. L.; Suchanski, N. R.; Wallace, W. L. and Cape, T.; Abstracts: 149th Meeting of the Electrochem. Soc., Washington, D. C., May 6, 1976, Abs. No. 357.

[3] Fleischmann, M.; Hendra, P. J.; and McQuillan, A. J., J. Chem. Soc. Chem. Commun., 1973, 80.

[4] Little, L. H.; "Infrared Spectra of Adsorbed Species," Academic Press, New York, 1966.

[5] Hendra, P. J.; Horder, T. R. and Loader, E. J., J. Chem. Soc. A, 1971, 766.

[6] Fleischmann, M.; Hendra, P. J. and McQuillan, A. J., Chemical Physics Lett., 1974, 26, 163.

[7] Jeanmaire, D. J. and Van Duyne, R. B., J. Electroanal. Chem., 1977, 84, 1.

[8] Adamson, A. W., "Physical Chemistry of Surfaces," Jo.. Wiley and Sons, N. Y., 1976.

[9] Harrick, N. J. and Beckman, K. H. in "Characterization of Solid Surfaces," Kane, P. F. and Larrabee, G. B. eds., Plenum Press, N. Y., 1976.

[10] Van Duyne, R. P.; J. Phys. (Paris), 1977, 38, 15.

[11] Dornhaus, R.; Long, M. B.; Benner, R. E.; and Chang, R. K.; Surf. Science, 1980, 93, 240.

[12] Van Duyne, R. P., "Chemical and Biochemical Applications of Lasers," Vol. 4, Ch. 5, C. B. Moore, Ed., 1979.

[13] Evans, J. F.; Albrecht, M. G.; Ullevig, D. M.; and Hexter, R. M.; J. Electroanal. Chem., 1980, 106, 209.

[14] Rowe, J. E.; Shank, C. V.; Zwemer, D. A. and Murray, C. A., submitted to Phys. Rev. Lett., 1980.

[15] Creighton, J. A.; Blatchford, D. G. and Albrecht, M. G., J. Chem. Soc. Faraday Trans. II, 1979, 75, 790.

[16] Pettinger, B. and Wenning, U.; Chem. Phys. Lett., 1978, 56, 253.

[17] Pettinger, B.; Wenning, U. and Kolb, D.; Ber. Bunsenges. Phys. Chem., 1978, 82, 1326.

[18] Pettinger, B. and Wenning, U.; Proceedings of the Conference on Vibrations in the Adsorbed Layer, Julich, Germany, 1978.

[19] Barradas, R. G. and Conway, B. E., J. Electroanal. Chem., 1963, 6, 314.

[20] Erdheim, G. E.; unpublished work, 1979.

[21] Regis, A. and Corset, J., Chem. Phys. Lett., 1980, 70, 305.

[22] Venkatesan, S.; Erdheim, G.; Lombardi, J. R. and Birke, R. L., to be published in Surface Science, 1980.

[23] Creighton, J.; Albrecht, M.; Hester, R. and Matthew, J., Chem. Phys. Lett., 1978, 55, 55.

[24] Allen, C. S.; Schultz, S. and Parks, K.; Chem. Phys. Lett., submitted 1978.

[25] Pettinger, B.; Tadjeddine, A. and Kolb, D. M., Chem. Phys. Lett., 1979, 66, 544.

[26] Wenning, U.; Pettinger, B. and Wetzel, H.; Chem. Phys. Lett., 1980, 70, 49.

[27] Albrecht, M. G., Evans, J. F. and Creighton, J. A., Surf. Sci., 1978, 75, L777.

[28] Smardzewski, R. R.; Colton, F. J. and Murday, J. S., Chem. Phys. Lett., 1979, 68, 53.

[29] Murray, C. A., personal communication.

[30] Bergman, J. G.; Heritage, J. P.; Pinzak, A.; Worlock, J. M. and McFee, J. H., Chem. Phys. Lett., .1979, 68, 412.

[31] Otto, A., Surf. Sci., 1978, 75, 392.

[32] Mahoney, M. R.; Howard, M. W. and Cooney, R. P., Chem. Phys. Lett., 1980, 71, 59.

[33] Heritage, J. P.; Bergman, J. G., Pinczuk, A. and Worlock, J. M., Chem. Phys. Lett., 1980,

[34] Pettinger, B., Chem. Phys. Lett., 1979, 67, 229.

[35] Lombardi, J. R. and Birke, R. L., Surf. Sci., in press.

[36] Erdheim, G. E., Birke, R. L. and Lombardi, J. R., Chem. Phys. Lett., 1980, 69, 3.

[37] Grossman, W. E.; Hester, R. E. and Girling, R. B., preprint.

[38] King, F. W.; Van Duyne, R.P. and Schatz, G. C., J. Chem. Phys., 1978, 69, 4472.

[39] Efrima, S. and Metiu, H., Chem. Phys. Lett., 1978, 60, 59; J. Chem. Phys., 1979, 70, 1602, 1939 and 2297.

[40] Eesley, G. L. and Smith, J.R., Solid State Commun., 1979, 31, 815.

[41] Hilton, P. R. and Oxtaby, D. W., submitted to J. Chem. Phys., 1980.

[42] Otto, A. in: Proc. Intern. Conf. on Vibrations in Adsorbed Layers, Julich, 1978.

[43] McCall, S. L. and Platzman, P. M., Bull. Am. Phys. Soc., 1979, 24, 340.

[44] Philpott, M. R., J. Chem. Phys., 1975, 62, 1812.

[45] Efrima, S. and Metiu, H., J. Chem. Phys., 1979, 70, 1939 and Surface Sci., 1980, 92, 433.

[46] King, F. W. and Schatz, G.C., Chem. Phys., 1979, 38, 245.

[47] A review on this subject is given by R. R. Chance, A. Prock and Sibley in Advances in Chemical Physics, v. 37, Eds. I. Prigogine and S. Rice, 1978, 1.

[48] Moskovits, M., J. Chem. Phys., 1978, 69, 4159.

[49] Hexter, R. M. and Albrecht, M. G., Spectrochim. Acta 35A, 1979, 233.

[50] Creighton, J. A.; Blatchford, C. G. and Albrecht, M. G., J. Chem. Soc. Faraday II, to be published.

[51] Gersten, J. and Nitzan, A., J. Chem. Phys., to be published.

[52] Mie, G., Ann. Physik, 1908, 25, 377. Maxwell-Garnett, J. C., Phil. Trans. Roy. Soc. London, 1904, 203, 385 and 1906, 205, 237.

[54] Gersten, J. I.; Birke, R. L. and Lombardi, J. R., Phys. Rev. Letters, 1979, 43, 147.

[55] Burstein, E.; Chen, Y. J.; Chen, C. Y.; Lundquist, S. and Tosatti, E., Solid State Commun., 1979, 29, 567.

[56] Fuchs, R., Bull. Am. Phys. Soc. 1979, 24, 339.

[57] Chen, C. Y.; Burstein, E. and Lundquist, S., Solid State Comm., 1979, 32, 63.

[58] Murray, C. A., paper given at Am. Phys Soc. meeting, Ap. 1980.

[59] Long, D. A., and George, W. O., Spectrochim. Acta, 1963, 19, 1777.

[60] Allen, E. S. and Van Duyne, R. P., Chem. Phys. Lett., 1979, 63, 455.

[61] Bunding, K. A., Lombardi, J. R. and Birke, R. L., to be published, Chem. Phys.

[62] Clark, R. J. H., and Williams, C. S., Inorg. Chem., 1965, 4, 350.

[63] Medhi, K. C. and Mukherjee, D. K., Spectrochim. Acta., 1965, 21, 895.

[64] Fleischmann, M., Hendra, P. J., McQuillan, A. J., Paul, R. L. and Reid, E. S., Journal of Raman Spectroscopy, 1976, 4, 269.

[65] Takenaka, T., Adv. in Colloid and Interface Sci., 1979, 11, 291.

[66] Snyder, R. G. and Schachtschneider, J. H., Spectrochim. Acta, 1963, 19, 85.

[67] Conway, B. E., Matheson, J. G., and Dhar, D. P., J. Phys. Chem., 1974, 78, 1226.

[68] Conway, B. E. and Gordon, L. G. M., J. Phys. Chem., 1969, 73, 3609.

[69] Dornhaus, R. and Chang, R. K., Preprint.

[70] Bunding, K. A., Birke, R. L. and Lombardi, J. R., Unpublished results.

[71] Tsang, J. C. and Kirtley, J. R., Phys. Rev. Lett., 1979, 43, 772.

[72] Kabayashi, T., Spectrochim. Acta, 1970, 26 A, 1313 and 1939.

[73] Furtak, T., Trott, G. and Loo, B., Surface Sci., in press, 1980.

[74] Billmann, J., Kovacs, G. and Otto, A., Surface Sci., in press, 1980.

[75] Naman, R., private communication.

[76] Tomilov, A. P.; Maironovskii, S. G.; Fioshin, M. Ya. and Smirnov, V. A., "The Electrochemistry of Organic Compounds," John Wiley and Sons, New York. 1972.

[77] Allen, M. J. and Cahen, H., J. Electrochem. Soc., 1959, 106, 451.

[78] Brewster, J. H., J. Am. Chem. Soc., 1954, 76, 6361.

[79] Bencze, W. L. and Allen, J. J., J. Am. Chem. Soc., 1959, 81, 4015.

[80] Taylor, R., J. Chem. Soc., 1962, 4881.

[81] Freifelder, M., J. Org. Chem., 1964, 229, 2895.

[82] Bunding, K. A., unpublished results.

[83] Pocker, Y.; Meany, J. E. and Nist, B. J., J. Phys. Chem., 1967, 71, 4509.

[84] Schrader, B., "Raman/IR atlas Organischer Verbindingun," Verlag Chemie, Weinheim, V. 1-2, 1975.

[85] Varsanyi, G., "Assignments for Vibrational Spectra of 700 Benzene Derivatives," John Wiley and Sons, N. Y., V. 1-2, 1974.

[86] Lombardi, J. R., unpublished calculations.